Article

Thiosulfonylation of Unactivated Alkenes with Visible-Light Organic Photocatalysis

Karthik Gadde, Pieter Mampuys, Andrea Guidetti, HongYue Vincent Ching, Wouter A. Herrebout, Sabine Van Doorslaer, Kourosch Abbaspour Tehrani, and Bert U. W. Maes

ACS Catal., **Just Accepted Manuscript** • DOI: 10.1021/acscatal.0c02159 • Publication Date (Web): 23 Jun 2020

Thiosulfonylation of Unactivated Alkenes with Visible-Light Organic Photocatalysis

Karthik Gadde,[‡] Pieter Mampuys,[‡] Andrea Guidetti,[†] H.Y. Vincent Ching,[†] Wouter A. Herrebout,[£] Sabine Van Doorslaer,[†] Kourosch Abbaspour Tehrani,[‡] Bert U.W. Maes[,‡]*

[‡] Division of Organic Synthesis, Department of Chemistry, University of Antwerp, Groenenborgerlaan 171, B-2020 Antwerp, Belgium

[†] Biophysics and Biomedical Physics (BIMEF), Department of Chemistry, University of Antwerp, Universiteitsplein 1, B-2610 Antwerp, Belgium

[£] Molecular Spectroscopy, Department of Chemistry, University of Antwerp, Groenenborgerlaan 171, B-2020 Antwerp, Belgium

KEYWORDS: *Visible-light photocatalysis, Organic photocatalyst, Thiosulfonates, Difunctionalization, Energy Transfer.*

ABSTRACT

A metal-free method for the vicinal thiosulfonylation of unactivated alkenes with thiosulfonates using 9-mesityl-10-methylacridinium perchlorate as photo-organocatalyst with visible-light irradiation has been developed. The method can be performed in dimethyl carbonate under air at room temperature and features a broad functional group compatibility. Metrics indicate the *green potential* of the developed *versus* the state-of-the-art methodologies. Mechanistic studies revealed no single electron transfer but involvement of an energy transfer from the excited photo-organocatalyst to thiosulfonate reactant, subsequently providing a sulfenyl and a sulfonyl radical *via* homolytic cleavage.

INTRODUCTION

Functionalization *via* an addition reaction on alkenes represents an attractive atom-economic transformation for the construction of complex organic molecules. While 1,2-hydrofunctionalization[1] already received a lot of attention, the corresponding 1,2-difunctionalization[2] has in comparison been far less studied, and especially 1,2-bis-heteroatom introduction.[3] *O*,*O*- (dioxygenation),[3a, 3b] *N*,*N*- (diamination),[3c] *O*,*N*- (oxyamination),[3d, 3e] and *X*,*N*- (haloamination[3f] and haloazidation[3g]) as well as *S*,*S*-difunctionalization[3h-k] have been reported. In the latter class, especially 1,2-thiosulfonylation of olefins has only rarely been explored (Scheme 1).[4] The installation of a sulfonyl (R^1SO_2-) and sulfenyl (R^2S-) moiety is of synthetic interest as these functionalities appear in natural

products, bioactive molecules and pharmaceuticals (Figure 1).[5] Besides, sulfenyl and sulfonyl groups are attractive functionalities in organic synthesis as these are easily transformed into other functional groups,[6] such as alkenes *via* Julia olefination,[7] a Ramberg-Bäcklund reaction[8] or alkenylative cross-coupling.[9]

Figure 1: Examples of sulfonyl- (top) and sulfenyl-containing (bottom) active ingredients (AIs) of pharmaceuticals and agrochemicals.

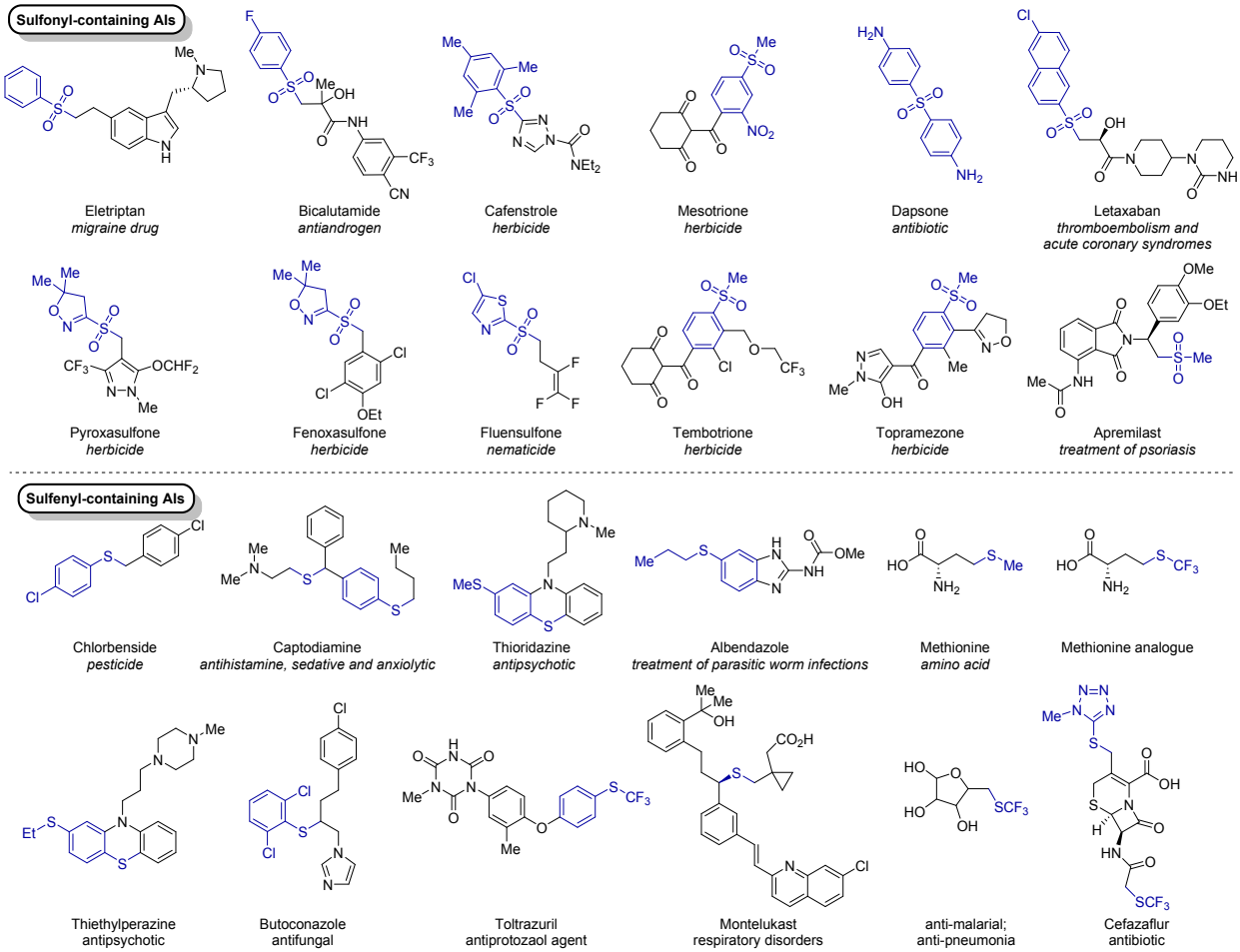

Recently, thiosulfonates ($R^1SO_2SR^2$)[10] have been disclosed as 1,2-thiosulfonylating reactants. Xu applied dual Au (IPrAuCl) and Ru ($Ru(bpy)_3Cl_2·6H_2O$) visible-light photoredox catalysis for the thiosulfonylation of styrenes (Scheme 1a).[4c] In this process $ArSO_2SR$ reacts with the Au catalyst and is not involved in the photoredox cycle. Later on, they reversed the

regioselectivity by employing a Sc Lewis acid catalyst ($Sc(OTf)_3$/bpy), favoring an ionic rather than a radical pathway (Scheme 1b).[4d] The first example of thiosulfonylation involving unactivated alkenes was reported by Shen, employing a silver nitrate catalyst and potassium persulfate as a stoichiometric oxidant (Scheme 1c).[4a, 4b] Unfortunately, the procedure only involved perfluoroalkyl benzenethiosulfonate reactants. Though pioneering from a synthetic organic chemistry point of view, these three procedures still show significant short comings with respect to *green chemistry*. They at least feature three of the following aspects: use of a (highly) hazardous solvent, a stoichiometric oxidant, a high loading of expensive and limitedly available rare-earth or noble metal based catalyst, an inert atmosphere. In addition, they are still limited in reactant scope, either to activated alkenes (e.g. styrenes) or perfluoroalkyl thiosulfonates. A general, mild, cheap and efficient method for thiosulfonylation of unactivated alkenes with a broad thiosulfonate scope using a cheap and readily available catalyst which can be performed in a *green* solvent under air has not been reported so far. In continuation of our interest in thiosulfonates[11] and *green* synthetic methodology development, we envisioned unprecedented alkyl and aryl thiosulfonylation of unactivated alkenes *via* visible-light organic photocatalysis (Scheme 1d). Considering the high oxidation potential of unactivated aliphatic alkenes this is a challenging goal [styrenes (E_{ox} < 2.0 V) < trisubstituted alkenes (2.0 < E_{ox} < 2.2 V) < disubstituted alkenes (2.2 > E_{ox} >

2.4 V) mono substituted alkenes (E_{ox} > 2.4 V); potentials *vs.* saturated calomel electrode (SCE)].[12] Photocatalysis in organic synthesis is predominantly focused on the use of noble metal complexes (mainly iridium and ruthenium) as catalyst.[13] However, the use of organic chromophores[14] as catalyst is still far less explored and beneficial in terms of cost and *green* credentials and therefore our preferred option.

Scheme 1. Thiosulfonylation of alkenes: state-of-the-art metal catalysis versus organocatalysis.

(a) Dual Au/Ru catalysis (Xu, 2017)

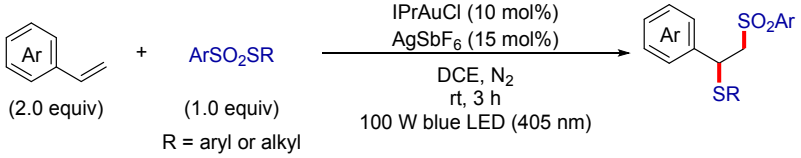

- ✗ Noble metal catalysts
- ✗ Highly hazardous solvent
- ✗ Inert atmosphere
- ✗ Limited to arenethiosulfonates
- ✗ High power LED required
- ✗ Limited to styrenes
- ✓ Visible light mediated
- ✓ Room temperature

(b) Sc-catalysis (Xu, 2019)

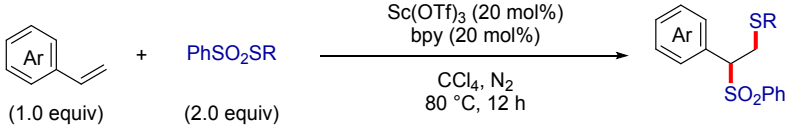

- ✗ Rare-earth metal catalyst
- ✗ Highly hazardous solvent
- ✗ Inert atmosphere
- ✗ Limited to benzenethiosulfonates
- ✗ Limited to styrenes
- ✓ Reverse regio-selectivity
- ✗ Reflux

(c) Ag-catalysis + $K_2S_2O_8$ (Shen, 2016)

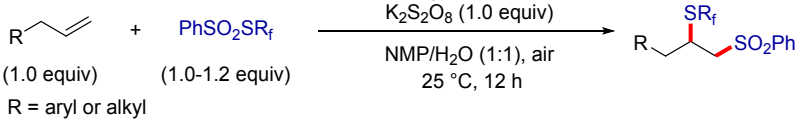

- ✗ Noble metal catalyst
- ✗ Hazardous solvent
- ✓ Air atmosphere
- ✗ Stoichiometric oxidant
- ✗ Limited to R_f benzenethiosulfonates
- ✓ Unactivated alkenes
- ✓ Room temperature

(d) This work (Metal-free): photo-organocatalysis

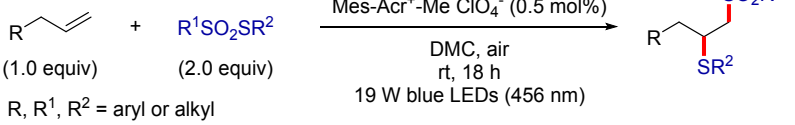

- ✓ Organocatalyst
- ✓ Green solvent
- ✓ Air atmosphere
- ✓ Alkyl and aryl thiosulfonates
- ✓ Unactivated alkenes
- ✓ Visible light mediated
- ✓ Room temperature

RESULTS AND DISCUSSION

We started our optimization with the reaction of allylbenzene (**1a**) and *S*-(4-methylphenyl) 4-methylbenzenethiosulfonate (**2a**) to give 1-methyl-4-([1-(4-methylbenzene-1-sulfonyl)-3-phenylpropan-2-yl]sulfanyl)benzene (**3a**) under visible light irradiation at room temperature (Table 1 and Supporting Information (SI) for detailed optimization studies). When 1 mol% of a frequently used noble metal-based photocatalyst,[13] $Ru(bpy)_3Cl_2 \cdot 6H_2O$, was applied only 9% of the desired product (**3a**) was obtained (Table 1, entry 1). This photocatalyst was also used for the thiosulfonylation of styrenes *via* dual catalysis applying a high power light-emitting diode (LED) (Scheme 1a).[4c] Clearly, completely different reaction conditions are required for efficient thiosulfonylation of unactivated alkenes under visible light. In accordance with our goal, a series of organic dyes, such as fluorescein, rose bengal, eosin Y, eosin B, rhodamine 6G, rhodamine B, and 9-mesityl-10-methylacridinium perchlorate [Mes-Acr^+-Me ClO_4^-] were subsequently evaluated as organic photocatalyst for the envisioned transformation (Table 1, entries 2–8).[14] Among them, Mes-Acr^+-Me ClO_4^- proved to be an efficient photocatalyst and **3a** was obtained in 54% yield (entry 8).[15] All other dyes furnished diminished yields (entries 2–5) or failed to deliver **3a** (entries 6 and 7). Interestingly, even a photocatalyst loading of 0.5 mol% proved still sufficient to obtain **3a** (entry 9). Raising the concentration from 0.1 M to 0.5 M allowed to achieve full conversion of

1a and delivered **3a** in 97% yield (entry 10). Pleasingly, the reaction could also be performed in air without significant loss of yield of **3a** (91%, entry 11). Next, solvents recommended based on *green* solvent guides were evaluated as alternative for *problematic* acetonitrile (entries 12–14).[16] Gratifyingly, *preferred* solvents isopropyl alcohol and dimethyl carbonate (DMC) furnished **3a** in 92% and 91% yield, respectively. DMC was chosen as the optimal solvent for the reaction and delivered **3a** in 89% isolated yield.[16] Omitting the photocatalyst or performing the reaction in the dark lead to no reaction, indicating their crucial role (entries 15, 17-18). Lowering the amount of **2a** to 1.5 equivalents was not beneficial for the yield of **3a** (entry 16).

Table 1. Reaction optimization on the model reaction of allylbenzene (**1a**) with *S*-(4-methylphenyl) 4-methylbenzenethiosulfonate (**2a**).[a]

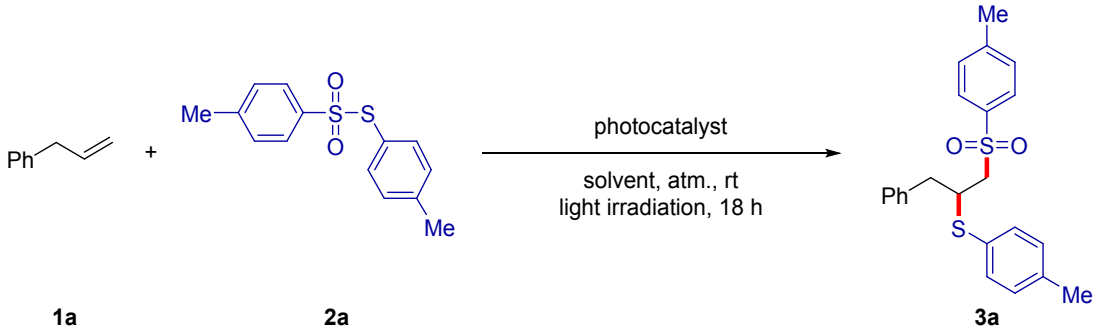

1a **2a** **3a**

Entry	Photocatalyst (mol%)	E_{red}^* (V)[b]	E_{ox}^* (V)[b]	Solvent (M) & Ranking[c]	Atm.	LED	Yield 3a [%][d]
1	$Ru(bpy)_3Cl_2·6H_2O$ (1.0)	+0.77	-0.81	CH_3CN (0.1)	Ar	Blue	9
2	Fluorescein (1.0)	+1.25	-1.55	CH_3CN (0.1)	Ar	Blue	12
3	Rose Bengal (1.0)	+0.81	-0.96	CH_3CN (0.1)	Ar	Green	23
4	Na_2-Eosin Y (1.0)	+0.83	-1.15	CH_3CN (0.1)	Ar	Blue	34
5	Eosin B (1.0)	+0.78	-1.37	CH_3CN (0.1)	Ar	Blue	23
6	Rhodamine 6G (1.0)	+1.18	-1.09	CH_3CN (0.1)	Ar	Blue	0
7	Rhodamine B (1.0)	+1.26	-1.31	CH_3CN (0.1)	Ar	Blue	0
8	Mes-Acr$^+$-Me ClO_4^- (1.0)	+2.08	/	CH_3CN (0.1)	Ar	Blue	54
9	Mes-Acr$^+$-Me ClO_4^- (0.5)	+2.08	/	CH_3CN (0.1)	Ar	Blue	65
10	Mes-Acr$^+$-Me ClO_4^- (0.5)	+2.08	/	CH_3CN (0.5)	Ar	Blue	97
11	Mes-Acr$^+$-Me ClO_4^- (0.5)	+2.08	/	CH_3CN (0.5)	Air	Blue	91
12	Mes-Acr$^+$-Me ClO_4^- (0.5)	+2.08	/	*i*-PrOH (0.5)	Air	Blue	92
13	Mes-Acr$^+$-Me ClO_4^- (0.5)	+2.08	/	EtOAc (0.5)	Air	Blue	55
14	**Mes-Acr$^+$-Me ClO_4^- (0.5)**	+2.08	**/**	**DMC (0.5)**	**Air**	**Blue**	**91 (89)[e]**
15	Mes-Acr$^+$-Me ClO_4^- (0.5)	+2.08	/	DMC (0.5)	Air	No[f]	0
16[g]	Mes-Acr$^+$-Me ClO_4^- (0.5)	+2.08	/	DMC (0.5)	Air	Blue	52
17	no photocatalyst	/	/	DMC (0.5)	Air	No[f]	0
18	no photocatalyst	/	/	DMC (0.5)	Air	Blue	5

[a] *Reaction conditions*: **1a** (0.25 mmol, 1.0 equiv), **2a** (0.50 mmol, 2.0 equiv), photocatalyst, solvent, atmosphere, rt, 18 h. Illumination by light-emitting diode (LED) strips (blue LED: λ_{max} = 456 nm or green LED: λ_{max} = 517 nm). [b] Excited state reduction potential (E_{red}*) and excited state oxidational potential (E_{ox}*) *vs.* saturated calomel electrode (SCE).[14b, 14c] More electrochemical data can be found in the Supporting Information.[c] Ranking according to the Chem21 solvent selection guide: amber denotes *problematic*, green denotes *recommended/preferred* solvent.[16] [d] ^{1}H NMR yield with 1,3,5-trimethoxybenzene as internal standard. [e] Isolated yield. [f] Reaction was performed in the dark. [g] 1.5 equiv of **2a** was used. EtOAc = ethyl acetate. DMC = dimethyl carbonate.

With the optimized conditions in hand [**1a** (0.5 mmol), **2a** (2.0 equiv), Mes-Acr^{+}-Me ClO_4^{-} (0.5 mol%), dimethyl carbonate (0.5 M), air, room temperature, 18 h and blue LED irradiation] the scope of the reaction was evaluated. First, *S*-(4-methylphenyl) 4-methylbenzenethiosulfonate (**2a**) was coupled with a variety of unactivated alkenes (**1**) (Table 2). Homoallylbenzene (**1b**) and hex-1-ene (**1c**) easily underwent 1,2-thiosulfonylation and the desired products (**3b** and **3c**) were isolated in excellent yield. Various functional groups on the alkene reactant, such as a halide (**1d**), alcohol (**1e**), ether (**1f**), imide (**1g**), ketone (**1h**), ester (**1i**), carboxylic acid (**1j** and **1k**) and nitrile (**1l**) did not effect this 1,2-thiosulfonylation reaction and the corresponding products (**3d–3l**) were obtained in good to excellent yield. Interestingly, acidic functional groups (alcohol (**1e**) and carboxylic acid (**1j** and **1k**)) were also tolerated. The substrates giving a low to moderate yield (**1f**, **1g**, and **1j**), performed better in acetonitrile under otherwise standard conditions. Allyltrimethylsilane (**1m**) was also successfully employed and furnished the corresponding product **3m** in moderate yield (42%). However, under these conditions also a small amount of desilylated product **3m′** (6%) was isolated. 1,4-Pentadiene (**1n**) was also smoothly converted into the corresponding mono-1,2-thiosulfonylated product **3n** in 49% yield and only a small amount (5%) of the bis-thiosulfonylated product **3n′** was isolated. Gratifyingly, 1,1-disubstituted terminal alkene such as 2-methyl-1-butene (**1o**) also afforded the desired product (**3o**) in

71% yield. Unfortunately, alkenes with low oxidation potential such as styrene did not deliver the desired 1,2-thiosulfonylation product. Oxidative sensitive electron-rich arenes, such as present in methyl eugenol (**1p**), gave only 9% target product **3p**. Extending the reaction time or altering of the solvent to acetonitrile did not significantly improve the yield in these cases. Interestingly, those substrates quench the excited acridinium photocatalyst, rationalizing the inhibition of the desired transformation (see SI, section 6.3.2). On the other hand, internal alkenes are surprisingly amenable to this reaction, as illustrated by 2-norbornene (**1q**), cyclohexene (**1r**), cyclopentene (**1s**), and 2,3-dihydrofuran (**1t**), which furnished the corresponding 1,2-thiosulfonylation products **3q–3t** in respectively 64%, 23%, 92% and 21% yield under standard reaction conditions. The yield of compounds **3r** and **3t** was improved to 65% and 51% by extending the reaction time to 48 h in dimethyl carbonate. Altering the solvent to acetonitrile, did not improve the yield here.

Table 2. Unactivated alkene (**1**) scope.[a]

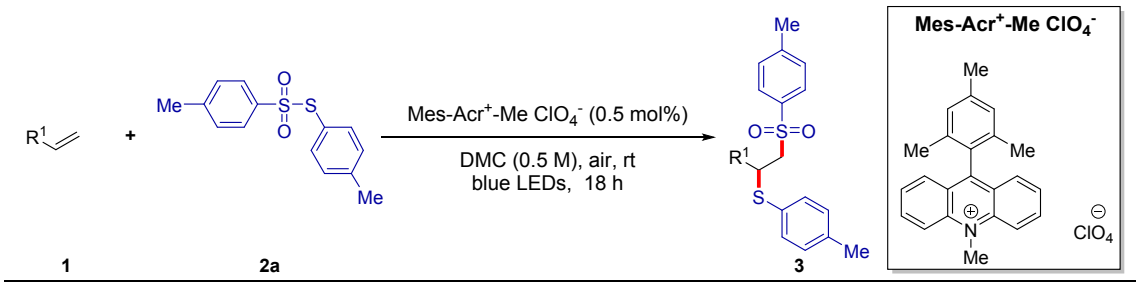

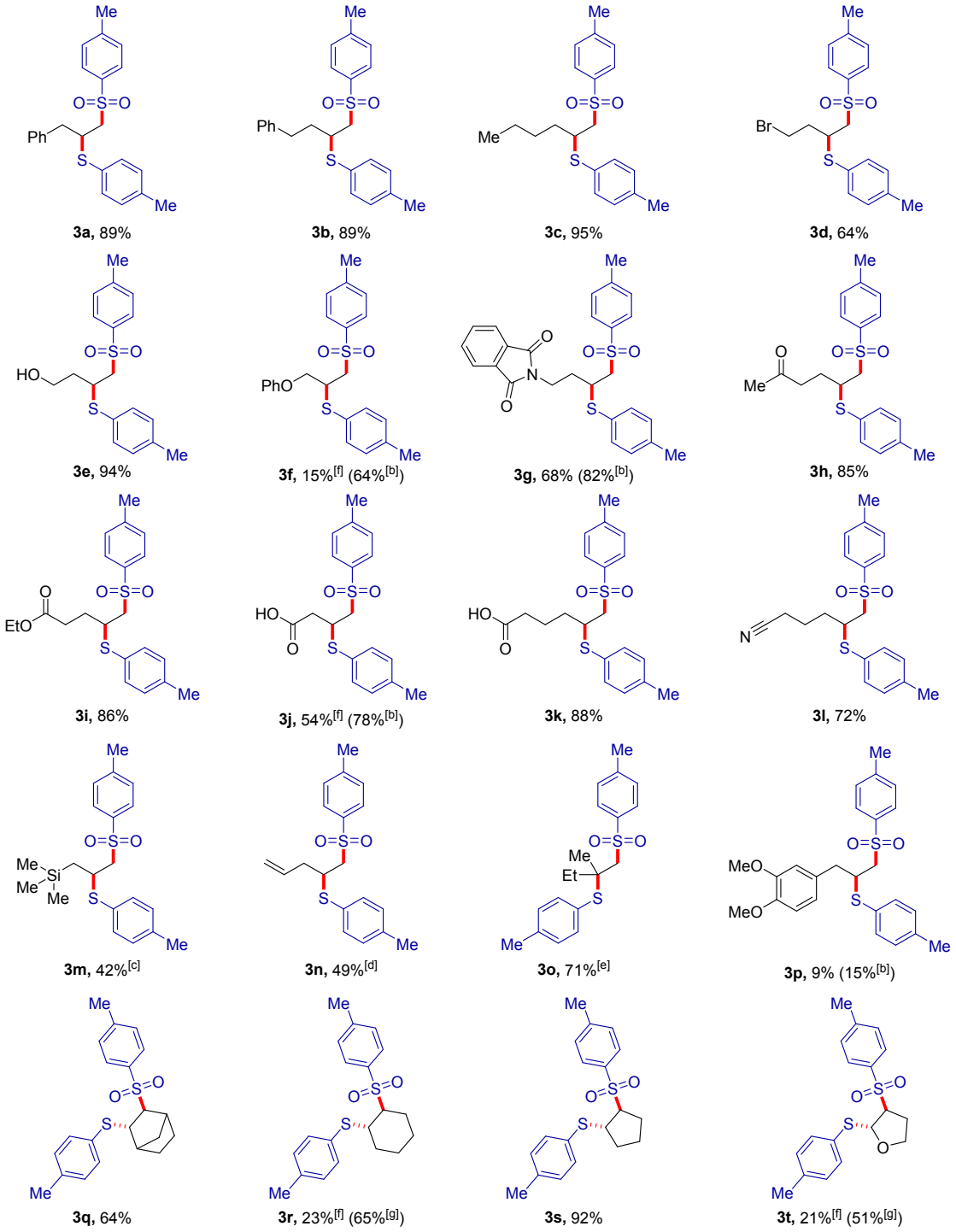

[a]*Reaction conditions*: **1** (0.5 mmol, 1.0 equiv), **2a** (1.0 mmol, 2.0 equiv), Mes-Acr$^+$-Me ClO_4^- (0.5 mol%), dimethyl carbonate (1.0 mL, 0.5 M), air, room temperature, 18 h, blue LEDs. Isolated yield unless indicated otherwise. [b] Reaction was conducted in acetonitrile (1.0 mL;

0.5 M). [c] 6% of the desilylated product **3m′** was obtained. [d] 5% of the bis-thiosulfonylated product **3n′** was obtained. [e] Reaction time 24 h. [f] ^{1}H NMR yield with 1,3,5-trimethoxybenzene as internal standard. [g] Reaction time: 48 h.

Our methodology could also successfully be applied on terminal aromatic and aliphatic alkynes (Scheme 2), without alteration of the reaction conditions.[17] Phenylacetylene (**5a**) and 1-ethynylcyclohexene (**5b**) reacted with *S*-(4-methylphenyl) 4-methylbenzenethiosulfonate (**2a**) and *S*-phenyl benzenethiosulfonate (**2d**) yielding the corresponding thiosulfonylation products **6a**, **6b**, **6c** and **6d** in 68%, 72%, 53% and 56% yield, respectively. Interestingly, in **5b** the acetylene reacted chemoselectively over the alkene.

Scheme 2. Aromatic and aliphatic terminal alkynes (**5a** and **5b**).

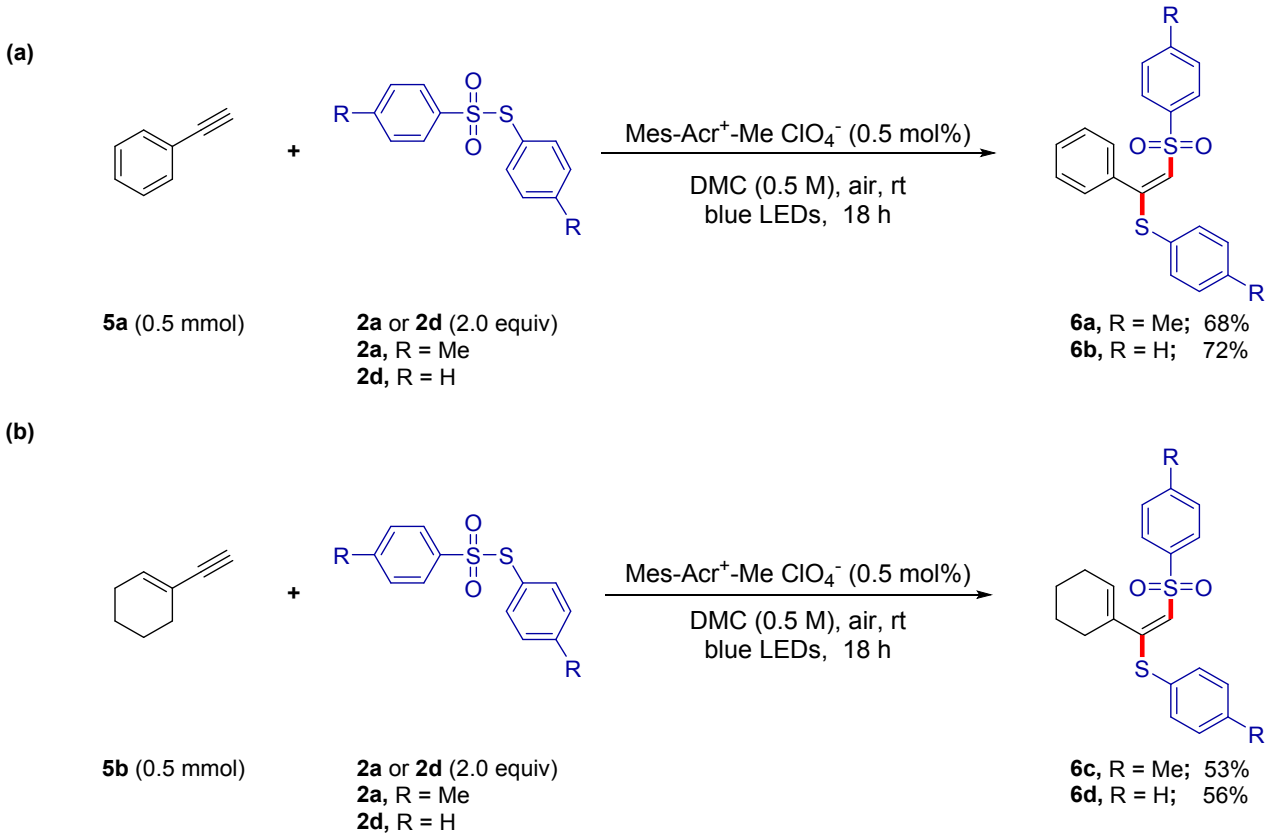

Next, the scope of the reaction with respect to the thiosulfonate (**2**) reactant was investigated with allylbenzene (**1a**) as the substrate (Table 3). Symmetrical ($R^1 = R^2$) *S*-aryl arenethiosulfonates, featuring substituents in different positions at the arene ring of the *S*-aryl arenethiosulfonate (**2b–2e**) were well tolerated (**3u–3x**). Heteroaromatic reactants can also be used as exemplified by *S*-thienyl thiophenethiosulfonate (**2f**), providing **3y** in 76% yield. Unsymmetrical *S*-aryl arenethiosulfonates ($R^1 \neq R^2$) (**2g–2i**) also generated the difunctional products (**3z–3ab**) in good to excellent yield. The protocol is also applicable to *S*-aryl alkanethiosulfonates and some *S*-alkyl arenethiosulfonates as exemplified by *S*-phenyl methanethiosulfonate (**2j**) and *S*-(trifluoromethyl) benzenethiosulfonate (**2k**), affording respectively **3ac** in 72% and **3ad** in 82% yield. Unfortunately, *S*-butyl benzenethiosulfonate (**2l**) did not convert towards the desired 1,2-thiosulfonation product **3ae**.

Table 3. Thiosulfonate (**2**) scope.[a]

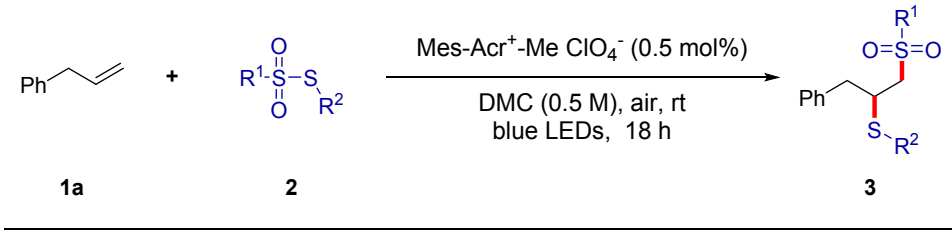

1a **2** **3**

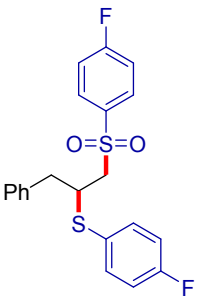

3u, 70%

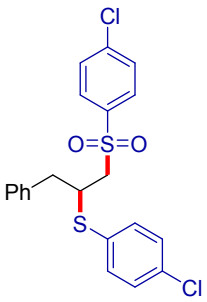

3v, 80%

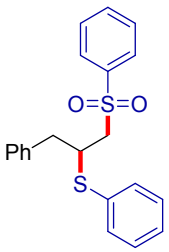

3w, 71%

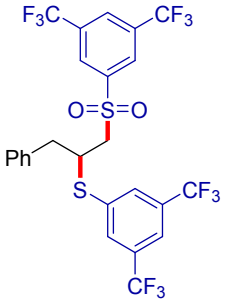

3x, 70%

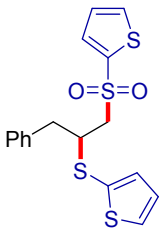

3y, 76%

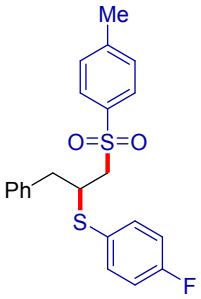

3z, 63%

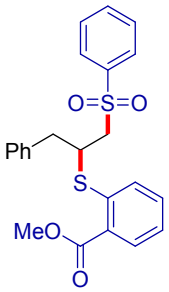

3aa, 84%

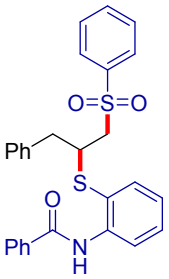

3ab, 90%

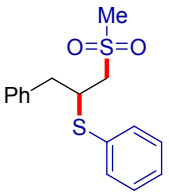

3ac, 13%[c] (72%[b])

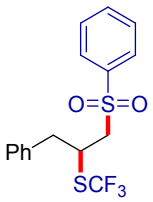

3ad, 82%

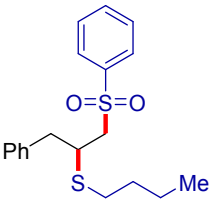

3ae, 0%

[a] *Reaction conditions*: **1a** (0.5 mmol, 1.0 equiv), **2** (1.0 mmol, 2.0 equiv), Mes-Acr^{+}-Me ClO_4^- (0.5 mol%), dimethyl carbonate (1.0 mL, 0.5 M), air, room temperature, 18 h, blue LEDs. Isolated yield unless indicated otherwise. [b] Reaction was conducted in acetonitrile (1.0 mL, 0.5 M). [c] ^{1}H NMR yield with 1,3,5-trimethoxybenzene as internal standard.

This methodology could also be extended to selenosulfonates, without adaptation of the reaction conditions, as exemplified by the reaction of *Se*-phenyl benzeneselenosulfonate (**2m**) with **1a** under standard conditions, giving the desired **7a** in 94% yield (Scheme 3).

Scheme 3. Application of *Se*-phenyl benzeneselenosulfonate (**2m**).

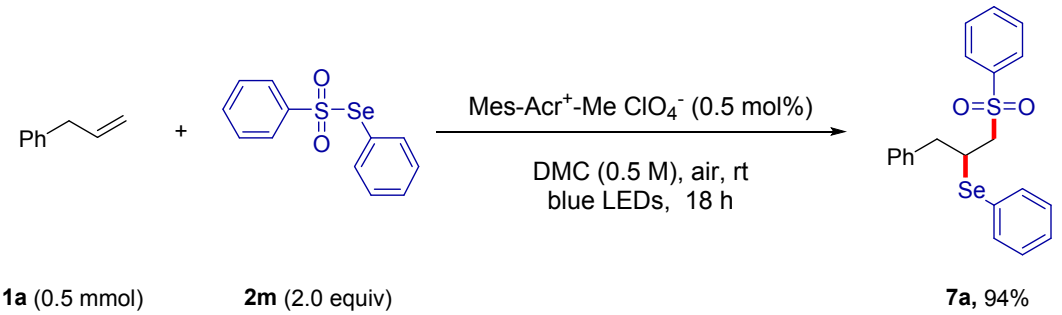

1a (0.5 mmol) **2m** (2.0 equiv) **7a,** 94%

When diallylether (**1u**) and diethyl diallylmalonate (**1v**) were subjected to the standard reaction conditions, cyclized products **8a** and **8b** were obtained in 95% and 84% yield, respectively (Scheme 4). While this 5-*exo*-*trig* cyclization is selectively occurring in 1,6-dienes, 1,2 addition is preferred over 3-*exo*-*trig* cyclization in 1,4-dienes (**3n**, Table 2).

Scheme 4. 5-*Exo*-trig cyclization in 1,6-dienes (**1u** and **1v**).

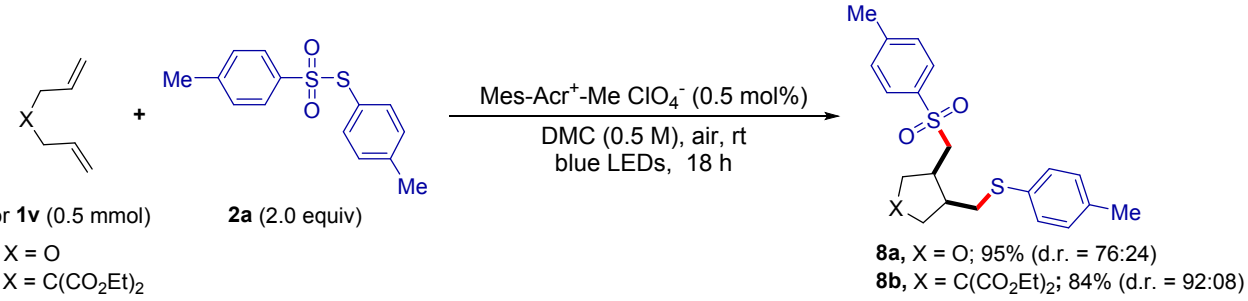

1u or **1v** (0.5 mmol) **2a** (2.0 equiv)

1u, X = O
1v, X = $C(CO_2Et)_2$

8a, X = O; 95% (d.r. = 76:24)
8b, X = $C(CO_2Et)_2$; 84% (d.r. = 92:08)

The robustness of our reaction was further studied *via* a toolkit recently developed by Glorius and co-workers.[18] Via a small number of experiments (SI, section 4) the reaction-condition-based sensitivity of our reaction was evaluated and the obtained results are visualized in Figure 2 *via* a color-coded radar diagram.[18] The studied parameters were concentration, water level, oxygen level, temperature, light intensity and scale of the

reaction. The resulting graph remains almost undeflected around the '0% deviation from standard yield line', except for low light intensity and high oxygen content. This medium sensitivity to light intensity is expected as the reaction is dependent on the excitation of the photocatalyst enabling crucial substrate excitation. With respect to oxygen sensitivity a negative effect (-17%) is observed when increasing oxygen concentration from air towards pure oxygen atmosphere, which of course has no practical meaning. Overall, a robust reaction has been developed.

Figure 2. Sensitivity assessment of the developed reaction towards concentration, water level, oxygen level, temperature, light intensity and scale, illustrated *via* a color-coded radar diagram as proposed by Glorius *et al.*[18] The deviation from standard reaction conditions is indicated as a black solid line. A round shape around the '0% deviation from standard line' indicates low sensitivity, any line deflecting from that to the red or green zones refer to high sensitivity of the reaction towards that parameter.

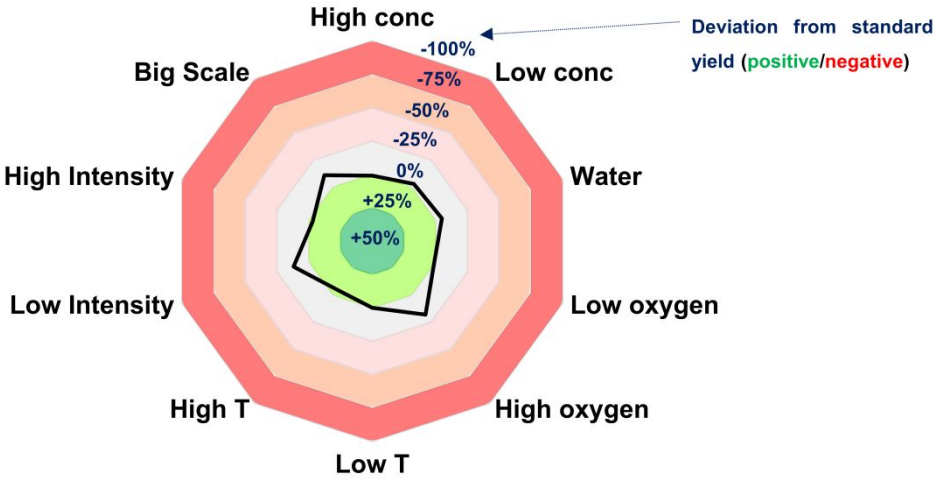

In order to appraise the *greenness* of the developed 1,2-thiosulfonylation approach, the CHEM21 Metrics Toolkit was employed.[19] This assessment is a relative concept considering

both quantitative and qualitative parameters. By comparing reported carefully selected examples of each methodology the *green potential* of the new *vs.* the state-of-the-art methodologies (Scheme 1) can be evaluated.[20] A detailed discussion of this evaluation can be found in the Supporting Information (section 5). Pleasingly, the results in Table 4 illustrate that the novel route has the largest *green potential* of the examined methodologies as it generates the lowest amount of waste (Process Mass Intensity (PMI) = 7.8 g g^{-1}). Moreover, for this route only green flags are obtained for important qualitative aspects of a reaction such as health and safety of reagents, energy use, solvent selection, and use of critical elements whereas multiple amber, red and brown flags are attributed to the three other routes.

Table 4. Appraisal of the *green* credentials of the different 1,2-thiosulfonylation approaches presented in Scheme 1.[a]

Method Scheme 1	PMI (g g^{-1})	Health and Safety[b]	Flag	Energy	Flag	Solvents	Flag	Critical elements	Flag
A (Xu)	22.2	DCE $AgSbF_6$ IPrAuCl $Ru(bpy)_3Cl_2$		rt		DCE		Au Sb Ag Ru	
B (Xu)	32.0	CCl_4 2,2-bipyridine $Sc(OTf)_3$		reflux		CCl_4		Sc	
C (Shen)	14.8	NMP $AgNO_3$ $K_2S_2O_8$ water		rt		NMP water		Ag	
D (this work)	7.8	DMC Mes-Acr$^+$-Me ClO_4^-		rt		DMC		none	

[a] Green flag denotes recommended (or preferred), amber flag denotes problematic, substitution preferred and red flag denotes hazardous (substitution is a priority) and brown flag denotes highly hazardous. [b] The health and safety flags from the reactants, *i.e.* **1** and **2**, have been omitted as only the *green* potential from the methodologies irrespective from the selected examples is appreciated. DCE = 1,2-dichloroethane. NMP = *N*-methyl-2-pyrrolidone. DMC = dimethyl carbonate.

Several experiments were conducted on the model reaction of **1a** and **2a** to gain insight in the reaction mechanism of our transformation (Schemes 5-6 & SI section 6). The radical nature of the reaction was confirmed by the addition of radical inhibitors to the model reaction. All tested radical inhibitors - TEMPO (2,2,6,6-tetramethylpiperidin-1-oxyl), galvinoxyl, and BHT (butylated hydroxytoluene) - completely inhibited the formation of 1-methyl-4-([1-(4-methylbenzene-1-sulfonyl)-3-phenylpropan-2-yl]sulfanyl)benzene (**3a**)

(Scheme 5a & SI section 6.5). Radical formation from thiosulfonate was further supported by irradiation a 1:1 mixture of *S*-(4-methylphenyl) 4-methylbenzenethiosulfonate (**2a**) and *S*-(4-fluorophenyl) 4-fluorobenzenethiosulfonate (**2b**) under optimal reaction conditions in the absence of allylbenzene (**1a**). Scrambled thiosulfonates **2g** and **2n** were obtained in 28% (Scheme 6a). Omitting the light or photocatalyst did not lead to the formation of **2g** and **2n** and both **2a** and **2b** were fully recovered (Scheme 6a). These results suggest the homolytic cleavage of the SO_2-*S* thiosulfonate bond under visible light irradiation in the presence of photocatalyst, thereby generating both a sulfonyl and a sulfenyl radical. Interestingly, when 1,2-bis-(4-fluorophenyl)disulfide (**4b**) was added to the model reaction a scrambled product **3z** was obtained in 37%, along with 50% of the desired product **3a** (Scheme 6b). This points to the involvement of a disulfide intermediate in the catalytic cycle. Also in this case no reaction was observed in the dark (Scheme 6b). When *S*-(4-methylphenyl) 4-methylbenzenethiosulfonate (**2a**) and 1,2-bis-(4-fluorophenyl)disulfide (**4b**) were brought under the standard reaction conditions in the absence of allylbenzene all possible thiosulfonates and disulfides were observed, fully in accordance with the thiosulfonate scrambling experiment (Scheme 6c).

Scheme 5. Control reactions to support mechanism.

(a) Radical inhibition experiment

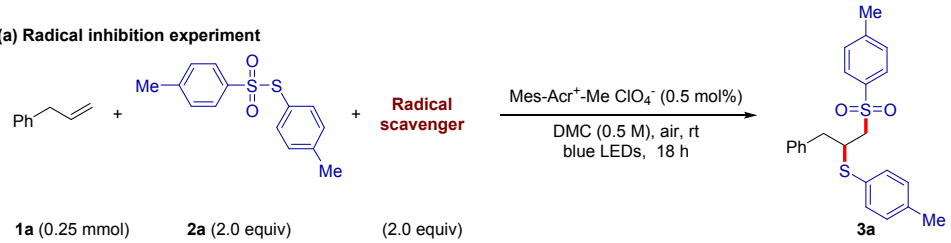

1a (0.25 mmol) **2a** (2.0 equiv) (2.0 equiv) **3a**

Radical scavenger	none	TEMPO	BHT	galvinoxyl
Yield of **3a** [%][a]	91	0	0	0

(b) Light-dark cycle experiment

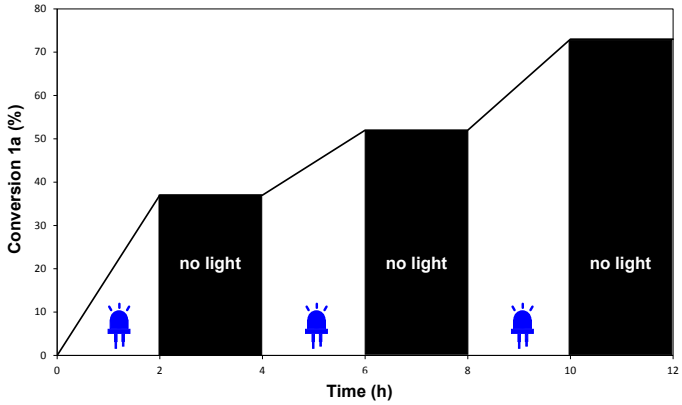

(c) UV LEDs experiment

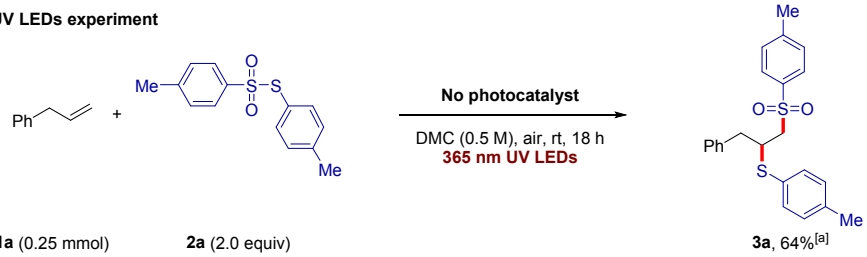

1a (0.25 mmol) **2a** (2.0 equiv) **3a**, 64%[a]

[a] ^{1}H NMR yield with 1,3,5-trimethoxybenzene as internal standard

Scheme 6. Scrambling experiments to support the reaction mechanism.

(a) Scrambling experiment between thiosulfonates 2a and 2b

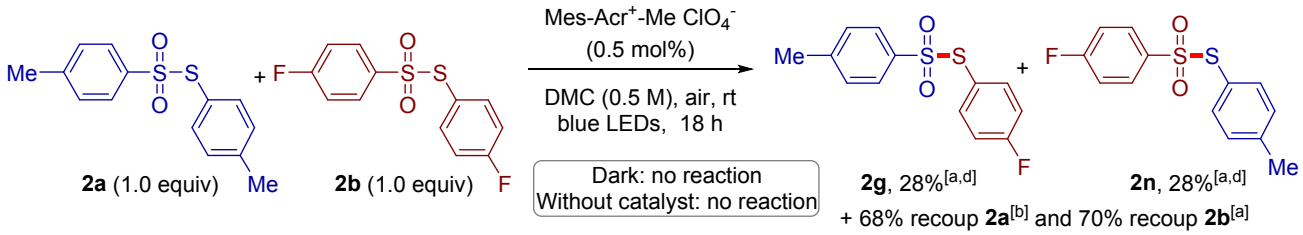

(b) Scrambling experiment on the model reaction with added disulfide 4b

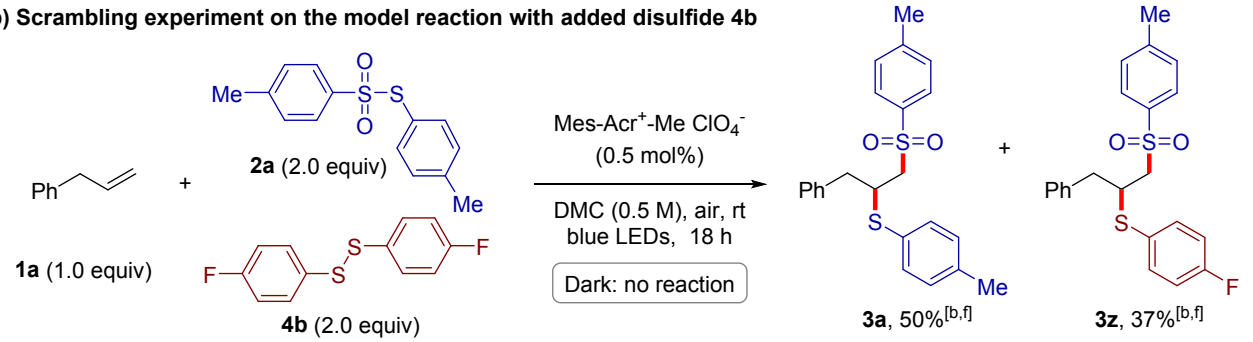

(c) Scrambling experiment between thiosulfonate 2a and disulfide 4b

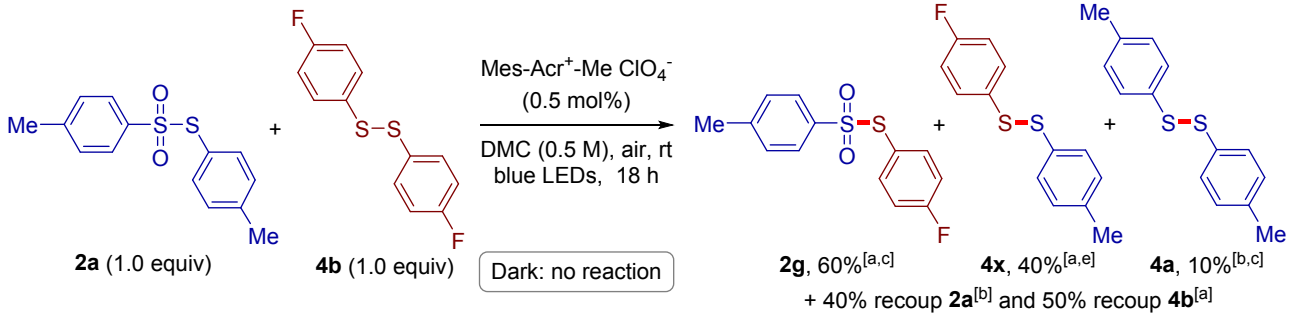

(d) Scrambling experiment between disulfides 4a and 4b

(e) Scrambling experiment between thiosulfonates 2a and 2l

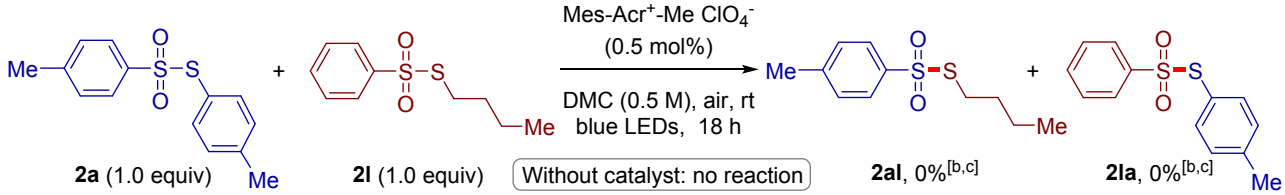

(f) Scrambling experiment between thiosulfonate 2a and disulfide 4l

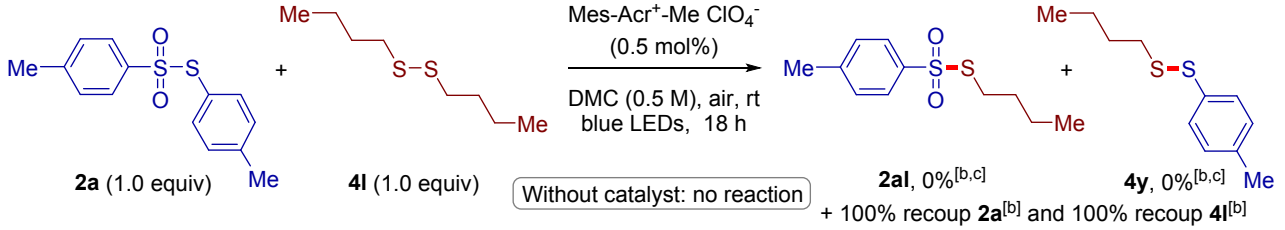

[a] ^{19}F NMR yield with hexafluorobenzene as internal standard [b] ^{1}H NMR yield with 1,3,5-trimethoxybenzene as internal standard
[c] Based on the amount of **2a** [d] Based on the amount of **2b** [e] Based on the amount of **4b** [f] Based on the amount of **1a**

Both allylbenzene (**1a**) and *S*-(4-methylphenyl) 4-methylbenzenethiosulfonate (**2a**) marginally absorb light above 400 nm as supported by UV-visible absorption spectra (SI, Figures S7-S8) in accordance with the observation that both visible light and the photocatalyst are essential for the reaction (Table 1, entries 15, 17–18). The acridinium salt [Mes-Acr^{+}-Me ClO_4^{-}] is the species in the reaction mixture absorbing the visible light photons efficiently (λ_{max1} = 359 nm, λ_{max2} = 420 nm, see SI Figure S6), hereby generating an excited state able to deliver radicals from the reactants. A 'light-dark cycle experiment' was subsequently conducted (Scheme 5b and SI section 6.8). The model reaction was completely inhibited in the absence of light and restarted when the light was turned back on. Although this intuitively points to no involvement of a radical chain - *i.e.* our transformation needs continuous irradiation of visible light to produce radicals - this type of experiment is not conclusive as reported by Yoon.[21] Indeed, a quantum yield of Φ = 1.9 was determined for the model reaction, employing the standard ferrioxalate actinometry (see SI section 6.4), which points to a combination of a photocatalytic transformation and a radical chain reaction.[21] However, as this value is close to 1, the photocatalytic route is likely the dominant pathway.

Subsequently, we looked into how radicals can be formed by reaction with the excited state of the photocatalyst. The redox properties of the excited photocatalyst, allylbenzene (**1a**),

and *S*-(4-methylphenyl) 4-methylbenzenethiosulfonate (**2a**) were therefore compared to check involvement of a single electron transfer (SET) mechanism. The photocatalyst Mes-Acr^{+}-Me ClO_4^- displays an excited state reduction potential (E_{red}*) of + 2.08 V (charge transfer singlet state) or + 2.18 V (locally excited singlet state) *vs.* SCE (in CH_3CN).[14b] The one-electron oxidation potential (E_{ox}) of **1a** was determined to be + 2.52 V *vs.* SCE (in CH_3CN; Figure S9) which is higher than the excited-state reduction potentials (E_{red}*) of the photocatalyst, eliminating a reductive quenching process. More substituted aliphatic alkenes and styrenes (conjugated) reduce the E_{ox} value, rationalizing the high oxidation potential measured for the unactivated mono substituted alkene **1a**.[12] *S*-(4-methylphenyl) 4-methylbenzenethiosulfonate (**2a**) can be easily reduced (-1.43 V *vs.* SCE in CH_3CN; Figure S10), but not oxidized.[22] SET from either **1a** and **2a** to the excited state of the photocatalyst is therefore excluded. Fluorescence quenching studies and a Stern-Volmer plot revealed that **2a** interacts with the excited organo-photocatalyst (Figures S13 - S15). This points to involvement of an energy transfer (EnT) mechanism.[23,24,25] Visible light-mediated energy transfer catalysis has remained a relatively underdeveloped field.[23] Interestingly, reported photocatalytic reactions with acridinium photocatalyst involving alkenes have only been reported to occur *via* the formation of the corresponding radical cations, subsequently trapped with suitable nucleophiles.[26]

Two energy transfer mechanisms are possible, i.e. Förster (*via* coulombic interaction) and Dexter (*via* exchange interaction). As no spectral overlap is observed between the emission spectrum of the donor (photocatalyst Mes-Acr$^+$-Me ClO_4^-; λ_{em} > 430 nm) and the UV-visible absorption spectrum of the acceptor **2a** (λ_{ab} < 350 nm); a Dexter rather than Förster EnT seems to be occurring (Figure S8). TD-DFT calculations on photocatalyst Mes-Acr$^+$-Me and *S*-(4-methylphenyl) 4-methylbenzenethiosulfonate (**2a**) support a triplet-triplet energy transfer (Figure S33).[24l] To further support involvement of an EnT, concomitantly producing two radicals, additional studies were performed. Electron paramagnetic resonance (EPR) experiments were conducted. DMPO (5,5-dimethyl-1-pyrroline *N*-oxide) was added to the model reaction in order to trap the radicals involved, which indeed revealed the presence of both a sulfenyl and a sulfonyl radical (Figure 3 & SI, section 6.9 for detailed EPR study). This is in accordance with the scrambling experiment of two thiosulfonates (Scheme 6a). Moreover, when the reaction was performed under UV light irradiation without a photocatalyst, the same reaction also occurred with the same regioselectivity (Scheme 5c). To exclude singlet oxygen ($^1O_2$) as quencher of our catalyst under air atmosphere, the production of $^1O_2$ was monitored *via* EPR using 2,2,6,6-tetramethylpiperidine as a trap (SI, section 6.10). However, no significant spectral changes to the blank reaction were observed, which therefore rules out $^1O_2$ involvement in our catalytic cycle.

Figure 3. DMPO spin-trapping experiment on the model reaction of **1a** and **2a**, continuous wave (cw) X-band (~9.44 GHz) EPR recorded at room temperature using 5 mW microwave power, 0.05 mT modulation amplitude and 100 kHz modulation frequency, and the individual components used for the spectral simulations. The ratio of R1 : R2 : R3 : Mes-Acr•-Me used for simulation was 1 : 0.9 : 0.6 : 6 (see SI section 6.9 for more details). Exp. = experimental spectrum. Sim. = simulated spectrum.

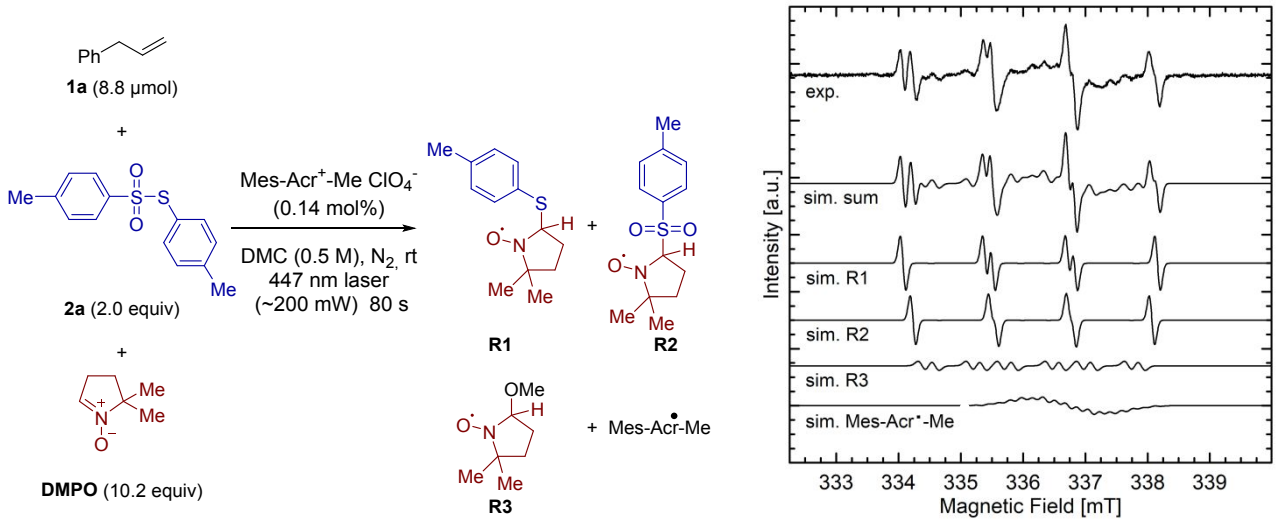

On the basis of the control experiments, both a photocatalytic and radical chain mechanism have been proposed for the model reaction, which are concomitantly occurring (Scheme 7). Initially, under irradiation with visible light, the photocatalyst Mes-Acr$^+$-Me ClO_4^- reaches an excited-state, i.e. [Mes-Acr$^+$-Me ClO_4^-]*, which then undergoes an energy transfer to *S*-(4-methylphenyl) 4-methylbenzenethiosulfonate (**2a**), regenerating ground state Mes-Acr$^+$-Me ClO_4^-, and excited *S*-(4-methylphenyl) 4-methylbenzenethiosulfonate (**2a***). Subsequently, **2a*** undergoes homolytic cleavage of the SO_2–*S* bond to afford a sulfenyl radical **A** and a sulfonyl radical **B**. Addition of radical **B** to allylbenzene (**1a**) generates intermediate **C**. Radical **C** can then react with sulfenyl radical **A** yielding target compound **3a** (photocatalysis). Radical **C** can also be involved in a radical chain process *via* reaction with

reactant **2a** generating product **3a** and radical **B**, which by reaction with allylbenzene (**1a**) can initiate another cycle. There is a second possible radical chain involving sulfenyl radical **A**, which could also react with thiosulfonate **2a**, hereby delivering 1,2-bis-(*p*-tolyl)disulfide (**4a**) and radical **B**. Addition of radical **B** to allylbenzene (**1a**) generates intermediate **C**, which then reacts with 1,2-bis-(*p*-tolyl)disulfide (**4a**) to furnish the desired product **3a** along with radical **A**. There is a driving force to rapidly form disulfide **4a** from **A**. Reported coulometric experiments on $PhSO_2SPh$ involving one electron reduction show the formation of PhSSPh and $PhSO_2^-$.[18a] In accordance with this, the calculated Bond Dissociation Energy (BDE) of **4a** is larger than the one of **2a** (BDE **4a** = 189.9 kJ mol^{-1} *vs.* BDE **2a** = 181.1 kJ mol^{-1}) (SI, Section 6.11). There is no driving force to form 1,2-bis-(*p*-tolyl)disulfone from sulfonyl radical **B** as the BDE is significantly lower (167.0 kJ mol^{-1}), rationalizing its reaction with allylbenzene (**1a**). **4a** does not need to react with radicals as blue light can split it into two sulfenyl radicals **A**.[26a,c-27] This is confirmed *via* a scrambling experiment of 1,2-bis-(*p*-tolyl)disulfide (**4a**) and 1,2-bis-(4-fluorophenyl)disulfide (**4b**) (Scheme 6d). While thiosulfonates need a photocatalyst to homolytically cleave with visible light, the corresponding disulfides do not (Scheme 6a and d). In addition, thiosulfonate **2a** does not scramble with *S*-butyl benzenethiosulfonate (**2l**) and 1,2-bis-(*n*-butyl)disulfide (**4l**) indicating their BDE is too high and the radicals A and B formed from **2a** just recombine (Scheme 6e

and f). This is in line with the reaction scope where *S*-butyl 4-methylbenzenethiosulfonate (**2l**) did not give reaction product **3ae** and no 1,2-bis-(*n*-butyl)disulfide (**4l**) formation was observed (Table 3).

Scheme 7. Proposed reaction mechanism for the model reaction of **1a** with **2a.**

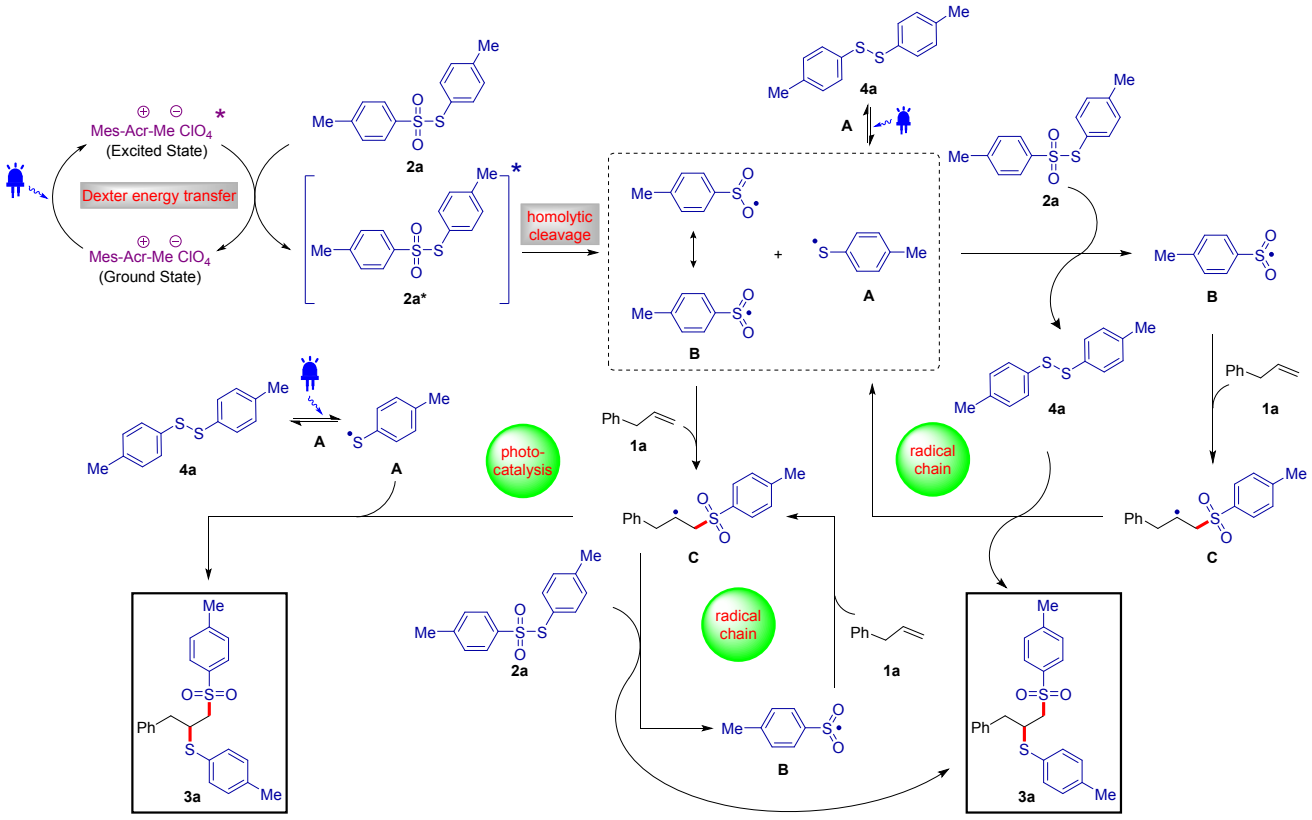

In order to demonstrate the synthetic utility of our protocol, a gram-scale reaction was carried out on our model system under standard reaction conditions (Scheme 8). Scaling up the reaction tenfold to 5 mmol allylbenzene substrate with *S*-(4-methylphenyl) 4-methylbenzenethiosulfonate (**2a**) reactant gave 1-methyl-4-([1-(4-methylbenzene-1-sulfonyl)-3-phenylpropan-2-yl]sulfanyl)benzene (**3a**) in 80% yield, which is only slightly lower

in comparison to the 0.5 mmol scale experiment (89%). The unreacted excess **2a** (1.29 g, 0.93 equiv, 93%) was also easily recovered during purification.

Scheme 8. Gram-scale synthesis of **3a** *via* thiosulfonylation of **1a** with **2a**.

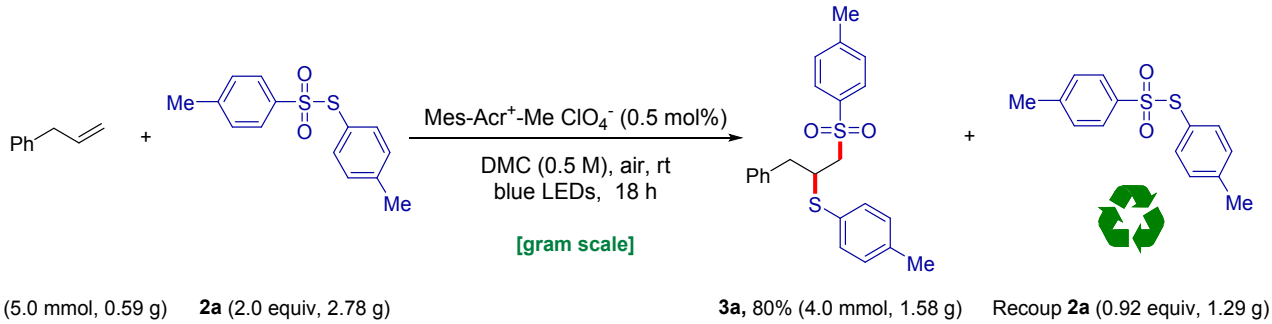

1a (5.0 mmol, 0.59 g) **2a** (2.0 equiv, 2.78 g) **3a,** 80% (4.0 mmol, 1.58 g) Recoup **2a** (0.92 equiv, 1.29 g)

As further illustration of the utility of our methodology, a direct diversification of an active pharmaceutical ingredient (API) has been attempted. Apronal (**1w**, hypnotic/sedative drug) was selected as model as it features NH /NH_2 groups of ureas and imides. Reaction of **1w** with **2a** provided target product **9a** in 79% yield (Scheme 9). This is remarkable as processes involving amidyl type radical formation in the *N*-acyl urea functionality were not observed. This further illustrates the chemoselectivity of the radical addition protocol developed.

Scheme 9. Synthetic Applications: thiosulfonylation of API Apronal (**1w**) with thiosulfonate **2a**.

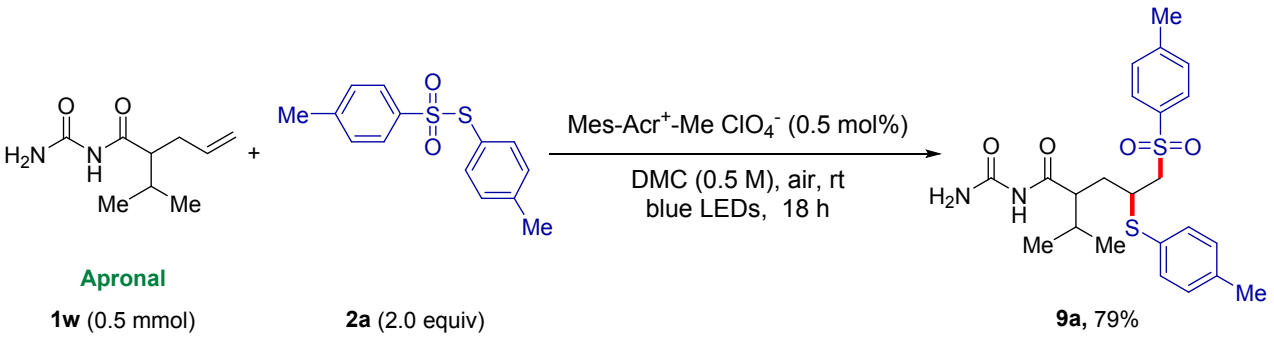

CONCLUSIONS

In summary, we have developed an organic dye photo-catalyzed method for vicinal thiosulfonylation of various unactivated alkenes with readily available thiosulfonates. This reaction represents a novel approach to concomitantly generate sulfonyl and sulfenyl radicals from thiosulfonates *via* energy transfer from visible light-excited 9-mesityl-10-methylacridinium perchlorate photo-organocatalyst. The method exhibits a broad reactant scope with an excellent functional group tolerance. Notably, the developed reaction is metal and oxidant free and can be conducted in a *green* solvent under air atmosphere and is applicable to the functionalization of olefins in APIs.

AUTHOR INFORMATION

Corresponding Author

* E-mail: bert.maes@uantwerpen.be

Author Contributions

The manuscript was written by Karthik Gadde, Pieter Mampuys and Bert U.W. Maes with contributions of all authors. All authors have given approval to the final version of the manuscript.

ASSOCIATED CONTENT

Supporting Information

The Supporting Information is available free of charge on the ACS Publications website.

Detailed optimization data, experimental procedures, characterization data, and copies of NMR spectra of all compounds (PDF).

ACKNOWLEDGMENTS

This work was financially supported by the Hercules and the Francqui Foundation, the University of Antwerp (BOF), H2020-MSCA-IF grant (grant number 792946, iSPY - H.Y.V. Ching) and the H2020-MSCA-EJD grant (grant number 813209, PARACAT, PhD student - A. Guidetti). The authors are grateful to Prof. Filip Lemière and Glenn Van Haesendonck for HRMS measurements, Prof. Tom Breugelmans and Filip Vorobjov for CV analysis, Prof. Christophe Vande Velde for X-ray analysis and Philippe Franck for the light reactors and HPLC analysis.

REFERENCES

1. For selected reviews dealing with 1,2-hydrofunctionalization of alkenes, see: a) Beller, M.; Seayad, J.; Tillack, A.; Jiao, H., Catalytic Markovnikov and anti-Markovnikov Functionalization of Alkenes and Alkynes: Recent Developments and Trends. *Angew. Chem. Int. Ed.* **2004**, *43*, 3368-3398; b) Hoffmann, R. W., Markovnikov Free Radical Addition Reactions, a Sleeping Beauty Kissed to Life. *Chem. Soc. Rev.* **2016**, *45*, 577-583; c) Dong, Z.; Ren, Z.; Thompson, S. J.; Xu, Y.; Dong, G., Transition-Metal-Catalyzed C–H Alkylation Using Alkenes. *Chem. Rev.* **2017**, *117*, 9333-9403; d) McAtee, R. C.; McClain, E. J.; Stephenson, C. R. J., Illuminating Photoredox Catalysis. *Trends in Chem.* **2019**, *1*, 111-125.

2. For selected reviews dealing with 1,2-difunctionalization of alkenes, see: a) Jensen, K. H.; Sigman, M. S., Mechanistic Approaches to Palladium-Catalyzed Alkene Difunctionalization Reactions. *Org. Biomol. Chem.* **2008**, *6*, 4083-4088; b) McDonald, R. I.; Liu, G.; Stahl, S. S., Palladium(II)-Catalyzed Alkene Functionalization *via* Nucleopalladation: Stereochemical Pathways and Enantioselective Catalytic Applications. *Chem. Rev.* **2011**, *111*, 2981-3019; c) Shimizu, Y.; Kanai, M., Recent Progress in Copper-Catalyzed Difunctionalization of Unactivated Carbon-Carbon Multiple Bonds. *Tetrahedron Lett.* **2014**, *55*, 3727-3737; d) Romero, N. A.; Nicewicz, D. A., Mechanistic Insight into the Photoredox Catalysis of Anti-Markovnikov Alkene Hydrofunctionalization Reactions. *J. Am. Chem. Soc.* **2014**, *136*, 17024-17035; e) Courant, T.; Masson, G., Recent Progress in Visible-Light Photoredox-Catalyzed Intermolecular 1,2-Difunctionalization of Double Bonds via an ATRA-Type Mechanism. *J. Org. Chem.* **2016**, *81*, 6945-6952.

3. For selected examples, see: a) Kolb, H. C.; VanNieuwenhze, M. S.; Sharpless, K. B., Catalytic Asymmetric Dihydroxylation. *Chem. Rev.* **1994**, *94*, 2483-2547; b) Bataille, C.

J. R.; Donohoe, T. J., Osmium-Free Direct S*yn*-Dihydroxylation of Alkenes. *Chem. Soc. Rev.* **2011**, *40*, 114-128; c) Muñiz, K.; Barreiro, L.; Romero, R. M.; Martínez, C., Catalytic Asymmetric Diamination of Styrenes. *J. Am. Chem. Soc.* **2017**, *139*, 4354-4357; d) Hemric, B. N.; Shen, K.; Wang, Q., Copper-Catalyzed Amino Lactonization and Amino Oxygenation of Alkenes Using *O*-Benzoylhydroxylamines. *J. Am. Chem. Soc.* **2016**, *138*, 5813-5816; e) Reed, N. L.; Herman, M. I.; Miltchev, V. P.; Yoon, T. P., Photocatalytic Oxyamination of Alkenes: Copper(II) Salts as Terminal Oxidants in Photoredox Catalysis. *Org. Lett.* **2018**, *20*, 7345-7350; f) Cai, Y.; Liu, X.; Zhou, P.; Kuang, Y.; Lin, L.; Feng, X., Iron-Catalyzed Asymmetric Haloamination Reactions. *Chem. Commun.* **2013**, *49*, 8054-8056; g) Seidl, F. J.; Min, C.; Lopez, J. A.; Burns, N. Z., Catalytic Regio- and Enantioselective Haloazidation of Allylic Alcohols. *J. Am. Chem. Soc.* **2018**, *140*, 15646-15650; h) Yamagiwa, N.; Suto, Y.; Torisawa, Y., Convenient Method for the Addition of Disulfides to Alkenes. *Bioorg. Med. Chem. Lett.* **2007**, *17*, 6197-6201; i) Wang, X.-R.; Chen, F., Iodine-Catalyzed Disulfidation of Alkenes. *Tetrahedron* **2011**, *67*, 4547-4551; j) Yadav, L. D. S.; Awasthi, C., The First One-Pot Oxidative 1,2-Acetoxysulfenylation and 1,2-Disulfenylation of Baylis–Hillman Alcohols in an Ionic Liquid. *Tetrahedron Lett.* **2009**, *50*, 3801-3804; k) He, R.; Chen, X.; Li, Y.; Liu, Q.; Liao, C.; Chen, L.; Huang, Y., NH_4I-Promoted and H_2O-Controlled Intermolecular Bis-Sulfenylation and Hydroxysulfenylation of Alkenes via a Radical Process. *J. Org. Chem.* **2019**, *84*, 8750-8758.

4. a) Zhu, D.; Shao, X.; Hong, X.; Lu, L.; Shen, Q., $PhSO_2SCF_2H$: A Shelf-Stable, Easily Scalable Reagent for Radical Difluoromethylthiolation. *Angew. Chem. Int. Ed.* **2016**, *55*, 15807-15811; b) Zhao, Q.; Lu, L.; Shen, Q., Direct Monofluoromethylthiolation with *S*-(Fluoromethyl) Benzenesulfonothioate. *Angew. Chem. Int. Ed.* **2017**, *56*, 11575-

11578; c) Li, H.; Shan, C.; Tung, C.-H.; Xu, Z., Dual Gold and Photoredox Catalysis: Visible Light-Mediated Intermolecular Atom Transfer Thiosulfonylation of Alkenes. *Chem. Sci.* **2017**, *8*, 2610-2615; d) Huang, S.; Li, H.; Xie, T.; Wei, F.; Tung, C.-H.; Xu, Z., Scandium-Catalyzed Electrophilic Alkene Difunctionalization: Regioselective Synthesis of Thiosulfone Derivatives. *Org. Chem. Front.* **2019**, *6*, 1663-1666.

5. a) Ilardi, E. A.; Vitaku, E.; Njardarson, J. T., Data-Mining for Sulfur and Fluorine: An Evaluation of Pharmaceuticals To Reveal Opportunities for Drug Design and Discovery. *J. Med. Chem.* **2014**, *57*, 2832-2842; b) Scott, K. A.; Njardarson, J. T., Analysis of US FDA-Approved Drugs Containing Sulfur Atoms. *Top. Curr. Chem.* **2018**, *376*, 5; c) Wang, N.; Saidhareddy, P.; Jiang, X., Construction of Sulfur-Containing Moieties in the Total Synthesis of Natural Products. *Nat. Prod. Rep.* **2020**, *37*, 246-275.
6. a) Trost, B. M.; Kalnmals, C. A., Sulfones as Chemical Chameleons: Versatile Synthetic Equivalents of Small-Molecule Synthons. *Chem. Eur. J.* **2019**, *25*, 11193-11213; b) *Sulphones in Organic Synthesis*. Pergamon Press Ltd.: Oxford, 1993; Vol. 10, 1-367.
7. a) Julia, M.; Paris, J.-M., Syntheses a l'Aide de Sulfones v(+)- Methode de Synthese Generale de Doubles Liaisons. *Tetrahedron Lett.* **1973**, *14*, 4833-4836; b) Wang, W.; Wang, B., Esterase-sensitive Sulfur Dioxide Prodrugs Inspired by Modified Julia Olefination. *Chem. Commun.* **2017**, *53*, 10124-10127.
8. a) Ramberg, L.; Bäcklund, B., *Arkiv Kemi Mineral. Geol.* **1940**, *13A*, 50; *Chem. Abstr.* **1940**, 34, 4725; b) Söderman, S. C.; Schwan, A. L., 1,2-Dibromotetrachloroethane: An Ozone-Friendly Reagent for the *in situ* Ramberg–Bäcklund Rearrangement and its Use in the Formal Synthesis of *E*-Resveratrol. *J. Org. Chem.* **2012**, *77*, 10978-10984.

9. Ishizuka, K.; Seike, H.; Hatakeyama, T.; Nakamura, M., Nickel-Catalyzed Alkenylative Cross-Coupling Reaction of Alkyl Sulfides. *J. Am. Chem. Soc.* **2010**, *132*, 13117-13119.

10. a) Mampuys, P.; McElroy, C. R.; Clark, J. H.; Orru, R. V. A.; Maes, B. U. W., Thiosulfonates as Emerging Reactants: Synthesis and Applications. *Adv. Synth. Catal.* **2020**, *362*, 3-64; b) Pannecoucke, X.; Besset, T., Use of $ArSO_2SR_f$ Reagents: an Efficient Tool for the Introduction of SR_f Moieties. *Org. Biomol. Chem.* **2019**, *17*, 1683-1693.

11. a) Mampuys, P.; Zhu, Y.; Vlaar, T.; Ruijter, E.; Orru, R. V. A.; Maes, B. U. W., Sustainable Three-Component Synthesis of Isothioureas from Isocyanides, Thiosulfonates, and Amines. *Angew. Chem. Int. Ed.* **2014**, *53*, 12849-12854; b) Mampuys, P.; Zhu, Y.; Sergeyev, S.; Ruijter, E.; Orru, R. V. A.; Van Doorslaer, S.; Maes, B. U. W., Iodide-Catalyzed Synthesis of Secondary Thiocarbamates from Isocyanides and Thiosulfonates. *Org. Lett.* **2016**, *18*, 2808-2811; c) Zhu, Y.-P.; Sergeyev, S.; Franck, P.; Orru, R. V. A.; Maes, B. U. W., Amine Activation: Synthesis of *N*-(Hetero)arylamides from Isothioureas and Carboxylic Acids. *Org. Lett.* **2016**, *18*, 4602-4605; d) Zhu, Y.-P.; Mampuys, P.; Sergeyev, S.; Ballet, S.; Maes, B. U. W., Amine Activation: *N*-Arylamino Acid Amide Synthesis from Isothioureas and Amino Acids. *Adv. Synth. Catal.* **2017**, *359*, 2481-2498; e) Mampuys, P.; Ruijter, E.; Orru, R. V. A.; Maes, B. U. W., Synthesis of Secondary Amides from Thiocarbamates. *Org. Lett.* **2018**, *20*, 4235-4239.

12. Roth, H. G.; Romero, N. A.; Nicewicz, D. A., Experimental and Calculated Electrochemical Potentials of Common Organic Molecules for Applications to Single-Electron Redox Chemistry. *Synlett* **2016**, *27*, 714-723.

13. a) Narayanam, J. M. R.; Stephenson, C. R. J., Visible Light Photoredox Catalysis: Applications in Organic Synthesis. *Chem. Soc. Rev.* **2011**, *40*, 102-113; b) Prier, C. K.; Rankic, D. A.; MacMillan, D. W. C., Visible Light Photoredox Catalysis with Transition Metal Complexes: Applications in Organic Synthesis. *Chem. Rev.* **2013**, *113*, 5322-5363; c) Reckenthäler, M.; Griesbeck, A. G., Photoredox Catalysis for Organic Syntheses. *Adv. Synth. Catal.* **2013**, *355*, 2727-2744; d) Arias-Rotondo, D. M.; McCusker, J. K., The Photophysics of Photoredox Catalysis: a Roadmap for Catalyst Design. *Chem. Soc. Rev.* **2016**, *45*, 5803-5820; e) Skubi, K. L.; Blum, T. R.; Yoon, T. P., Dual Catalysis Strategies in Photochemical Synthesis. *Chem. Rev.* **2016**, *116*, 10035-10074; f) Marzo, L.; Pagire, S. K.; Reiser, O.; König, B., Visible-Light Photocatalysis: Does It Make a Difference in Organic Synthesis? *Angew. Chem. Int. Ed.* **2018**, *57*, 10034-10072; g) Wang, C.-S.; Dixneuf, P. H.; Soulé, J.-F., Photoredox Catalysis for Building C–C Bonds from C(sp^2)–H Bonds. *Chem. Rev.* **2018**, *118*, 7532-7585; h) Kancherla, R.; Muralirajan, K.; Sagadevan, A.; Rueping, M., Visible Light-Induced Excited-State Transition-Metal Catalysis. *Trends in Chem.* **2019**, *5*, 510-523.

14. a) Nicewicz, D. A.; Nguyen, T. M., Recent Applications of Organic Dyes as Photoredox Catalysts in Organic Synthesis. *ACS Catal.* **2014**, *4*, 355-360; b) Romero, N. A.; Nicewicz, D. A., Organic Photoredox Catalysis. *Chem. Rev.* **2016**, *116*, 10075-10166; c) Bogdos, M. K.; Pinard, E.; Murphy, J. A., Applications of Organocatalysed Visible-Light Photoredox Reactions for Medicinal Chemistry. *Beilstein J. Org. Chem.* **2018**, *14*, 2035-2064.

15. a) Fukuzumi, S.; Kotani, H.; Ohkubo, K.; Ogo, S.; Tkachenko, N. V.; Lemmetyinen, H., Electron-Transfer State of 9-Mesityl-10-methylacridinium Ion with a Much Longer Lifetime and Higher Energy Than That of the Natural Photosynthetic Reaction Center.

J. Am. Chem. Soc. **2004**, *126*, 1600-1601; b) Benniston, A. C.; Harriman, A.; Li, P.; Rostron, J. P.; van Ramesdonk, H. J.; Groeneveld, M. M.; Zhang, H.; Verhoeven, J. W., Charge Shift and Triplet State Formation in the 9-Mesityl-10-methylacridinium Cation. *J. Am. Chem. Soc.* **2005**, *127*, 16054-16064. c) Fukuzumi, S.; Ohkubo, K.; Suenobu, T., Long-Lived Charge Separation and Applications in Artificial Photosynthesis. *Acc. Chem. Res.* **2014**, *47*, 1455-1464.

16. Prat, D.; Wells, A.; Hayler, J.; Sneddon, H.; McElroy, C. R.; Abou-Shehada, S.; Dunn, P. J., CHEM21 Selection Guide of Classical- and Less Classical-Solvents. *Green Chem.* **2016**, *18*, 288-296.

17. For thiosulfonylation of alkynes, see: a) Li, H.; Cheng, Z.; Tung, C.-H.; Xu, Z., Atom Transfer Radical Addition to Alkynes and Enynes: A Versatile Gold/Photoredox Approach to Thio-Functionalized Vinylsulfones. *ACS Catal.* **2018**, *8*, 8237-8243; b) Song, T. T.; Li, H. Y.; Wei, F.; Tung, C. H.; Xu, Z. H., Gold/Photoredox-Cocatalyzed Atom Transfer Thiosulfonylation of Alkynes: Stereoselective Synthesis of Vinylsulfones. *Tetrahedron Lett.* **2019**, *60*, 916-919; c) Reddy, R. J.; Kumari, A. H.; Kumar, J. J.; Nanubolu, J. B., Cs_2CO_3-Mediated Vicinal Thiosulfonylation of 1,1-Dibromo-1-Alkenes with Thiosulfonates: An Expedient Synthesis of (*E*)-1,2-Thiosulfonylethenes. *Adv. Synth. Catal.* **2019**, *361*, 1587-1591.

18. Pitzer, L.; Schäfers, F.; Glorius, F., Rapid Assessment of the Reaction-Condition-Based Sensitivity of Chemical Transformations. *Angew. Chem. Int. Ed.* **2019**, *58*, 8572-8576.

19. McElroy, C. R.; Constantinou, A.; Jones, L. C.; Summerton, L.; Clark, J. H., Towards a Holistic Approach to Metrics for the 21st Century Pharmaceutical Industry. *Green Chem.* **2015**, *17*, 3111-3121.

20. a) Abou-Shehada, S.; Mampuys, P.; Maes, B. U. W.; Clark, J. H.; Summerton, L., An Evaluation of Credentials of a Multicomponent Reaction for the Synthesis of Isothioureas Through the Use of a Holistic CHEM21 Green Metrics Toolkit. *Green Chem.* **2017**, *19*, 249-258; b) Monteith, E. R.; Mampuys, P.; Summerton, L.; Clark, J. H.; Maes, B. U. W.; McElroy, C. R., Why we Might be Misusing Process Mass Intensity (PMI) and a Methodology to Apply it Effectively as a Discovery Level Metric. *Green Chem.* **2020**, *22*, 123-135.

21. Cismesia, M. A.; Yoon, T. P., Characterizing Chain Processes in Visible Light Photoredox Catalysis. *Chem. Sci.* **2015**, *6*, 5426-5434.

22. a) Persson, B., Electrochemical Reduction of *S*-oxides of Diphenyl Disulfide: Part I. Investigation in Aprotic Solvents. *J. Electroanal. Chem.* **1978**, *86*, 313-323; b) Ji, C.; Ahmida, M.; Chahma, M. h.; Houmam, A., Radical/Ion Pair Formation in the Electrochemical Reduction of Arene Sulfenyl Chlorides. *J. Am. Chem. Soc.* **2006**, *128*, 15423-15431.

23. a) Strieth-Kalthoff, F.; James, M. J.; Teders, M.; Pitzer, L.; Glorius, F., Energy Transfer Catalysis Mediated by Visible Light: Principles, Applications, Directions. *Chem. Soc. Rev.* **2018**, *47*, 7190-7202; b) Zhou, Q.-Q.; Zou, Y.-Q.; Lu, L.-Q.; Xiao, W.-J., Visible-Light-Induced Organic Photochemical Reactions through Energy-Transfer Pathways. *Angew. Chem. Int. Ed.* **2019**, *58*, 1586-1604.

24. For selected recent examples, see: a) Teders, M.; Henkel, C.; Anhäuser, L.; Strieth-Kalthoff, F.; Gómez-Suárez, A.; Kleinmans, R.; Kahnt, A.; Rentmeister, A.; Guldi, D.; Glorius, F., The Energy-Transfer-Enabled Biocompatible Disulfide–Ene Reaction. *Nat. Chem.* **2018**, *10*, 981-988; b) Soni, V. K.; Lee, S.; Kang, J.; Moon, Y. K.; Hwang, H. S.; You, Y.; Cho, E. J., Reactivity Tuning for Radical–Radical Cross-Coupling *via* Selective

Photocatalytic Energy Transfer: Access to Amine Building Blocks. *ACS Catal.* **2019**, *9*, 10454-10463; c) Bellotti, P.; Brocus, J.; El Orf, F.; Selkti, M.; König, B.; Belmont, P.; Brachet, E., Visible Light-Induced Regioselective Cycloaddition of Benzoyl Azides and Alkenes To Yield Oxazolines. *J. Org. Chem.* **2019**, *84*, 6278-6285; d) Kudisch, M.; Lim, C.-H.; Thordarson, P.; Miyake, G. M., Energy Transfer to Ni-Amine Complexes in Dual Catalytic, Light-Driven C–N Cross-Coupling Reactions. *J. Am. Chem. Soc.* **2019**, *141*, 19479-19486; e) Ding, W.; Ho, C. C.; Yoshikai, N., Photosensitized, Energy-Transfer-Mediated Cyclization of 2-(1-Arylvinyl)benzaldehydes to Anthracen-9-(10*H*)-ones. *Org. Lett.* **2019**, *21*, 1202-1206; f) Patra, T.; Bellotti, P.; Strieth-Kalthoff, F.; Glorius, F., Photosensitized Intermolecular Carboimination of Alkenes through the Persistent Radical Effect. *Angew. Chem. Int. Ed.* **2020**, *59*, 3172-3177; g) Strieth-Kalthoff, F.; Henkel, C.; Teders, M.; Kahnt, A.; Knolle, W.; Gómez-Suárez, A.; Dirian, K.; Alex, W.; Bergander, K.; Daniliuc, C. G.; Abel, B.; Guldi, D. M.; Glorius, F., Discovery of Unforeseen Energy-Transfer-Based Transformations Using a Combined Screening Approach. *Chem* **2019**, *5*, 2183-2194; h) Ma, J.; Strieth-Kalthoff, F.; Dalton, T.; Freitag, M.; Schwarz, J. L.; Bergander, K.; Daniliuc, C.; Glorius, F., Direct Dearomatization of Pyridines via an Energy-Transfer-Catalyzed Intramolecular [4+2] Cycloaddition. *Chem* **2019**, *5*, 2854-2864; i) Xia, Z.; Corcé, V.; Zhao, F.; Przybylski, C.; Espagne, A.; Jullien, L.; Le Saux, T.; Gimbert, Y.; Dossmann, H.; Mouriès-Mansuy, V.; Ollivier, C.; Fensterbank, L., Photosensitized Oxidative Addition to Gold(I) Enables Alkynylative Cyclization of *O*-Alkylnylphenols with Iodoalkynes. *Nat. Chem.* **2019**, *11*, 797-805; j) Chen, D.-F.; Chrisman, C. H.; Miyake, G. M., Bromine Radical Catalysis by Energy Transfer Photosensitization. *ACS Catal.* **2020**, *10*, 2609-2614; k) Tian, L.; Till, N. A.; Kudisch, B.; MacMillan, D. W. C.; Scholes, G. D., Transient Absorption Spectroscopy

Offers Mechanistic Insights for an Iridium/Nickel-Catalyzed C–O Coupling. *J. Am. Chem. Soc.* **2020**, *142*, 4555-4559. (l) Xu, B.; Troian-Gautier, L.; Dykstra, R.; Martin, R. T.; Gutierrez, O.; Tambar, U. K., Photocatalyzed Diastereoselective Isomerization of Cinnamyl Chlorides to Cyclopropanes. *J. Am. Chem. Soc.* **2020**, *142*, 6206-6215. (m) Zhang, L.; Si, X.; Rominger, F.; Hashmi, S. K., Visible Light-Induced Radical Carbo-Cyclization/gem-Diborylation Through Triplet Energy Transfer between a Gold Catalysts and Aryl Iodides. *J. Am. Chem. Soc.* **2020**, *142*, 10485-10493.

25. For selected examples of acridinium photocatalyst used as photosensitizers, see: a) Crespin, L. N. S.; Greb, A.; Blakemore, D. C.; Ley, S. V., Visible-Light-Mediated Annulation of Electron-Rich Alkenes and Nitrogen-Centered Radicals from *N*-Sulfonylallylamines: Construction of Chloromethylated Pyrrolidine Derivatives. *J. Org. Chem.* **2017**, *82*, 13093-13108; b) Huang, L.; Rueping, M., Direct Cross-Coupling of Allylic C(sp^3)−H Bonds with Aryl- and Vinylbromides by Combined Nickel and Visible-Light Catalysis. *Angew. Chem. Int. Ed.* **2018**, *57*, 10333-10337.

26. a) Nguyen, T. M.; Manohar, N.; Nicewicz, D. A., Anti-Markovnikov Hydroamination of Alkenes Catalyzed by a Two-Component Organic Photoredox System: Direct Access to Phenethylamine Derivatives. *Angew. Chem. Int. Ed.* **2014**, *53*, 6198-6201; b) Gesmundo, N. J.; Grandjean, J.-M. M.; Nicewicz, D. A., Amide and Amine Nucleophiles in Polar Radical Crossover Cycloadditions: Synthesis of γ-Lactams and Pyrrolidines. *Org. Lett.* **2015**, *17*, 1316-1319; c) Margrey, K. A.; Nicewicz, D. A., A General Approach to Catalytic Alkene Anti-Markovnikov Hydrofunctionalization Reactions *via* Acridinium Photoredox Catalysis. *Acc. Chem. Res.* **2016**, *49*, 1997-2006.

27. Huang, W.; Chen, W.; Wang, G.; Li, J.; Cheng, X.; Li, G., Thiyl-Radical-Catalyzed Photoreductive Hydrodifluoroacetamidation of Alkenes with Hantzsch Ester as a Multifunctional Reagent. *ACS Catal.* **2016**, *6*, 7471-7474.

GRAPHICAL ABSTRACT

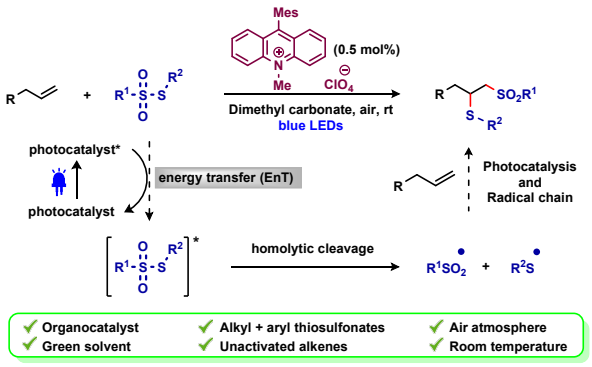

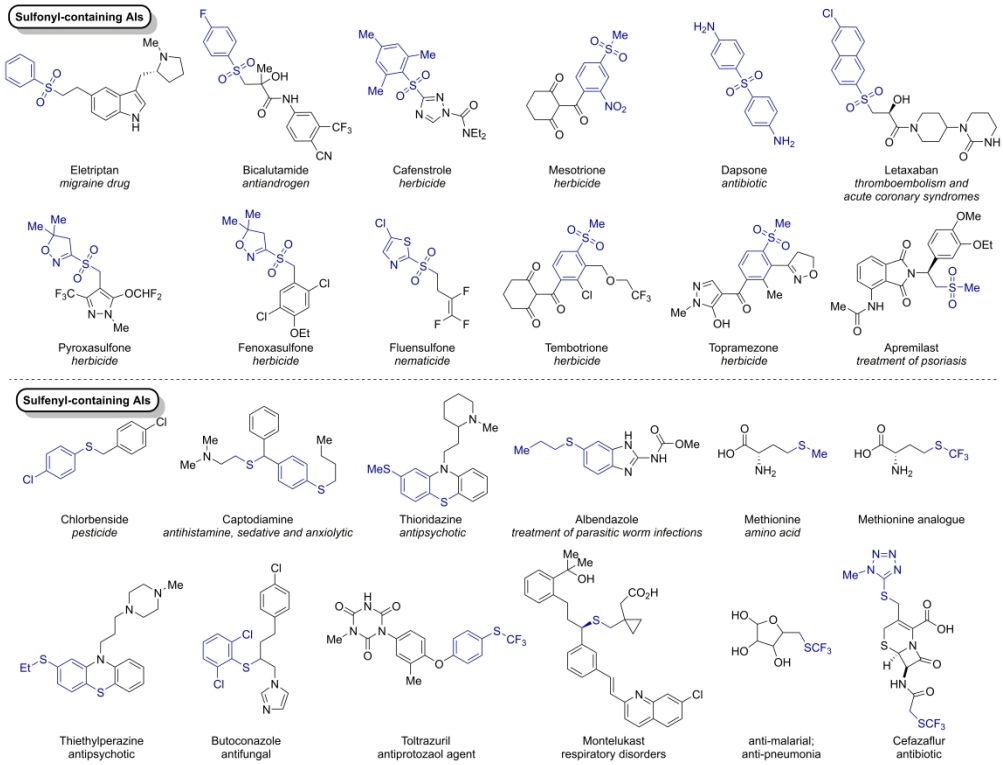

Figure 1. Examples of sulfonyl- (top) and sulfenyl-containing (bottom) active ingredients (AIs) of pharmaceuticals and agrochemicals.

306x233mm (600 x 600 DPI)

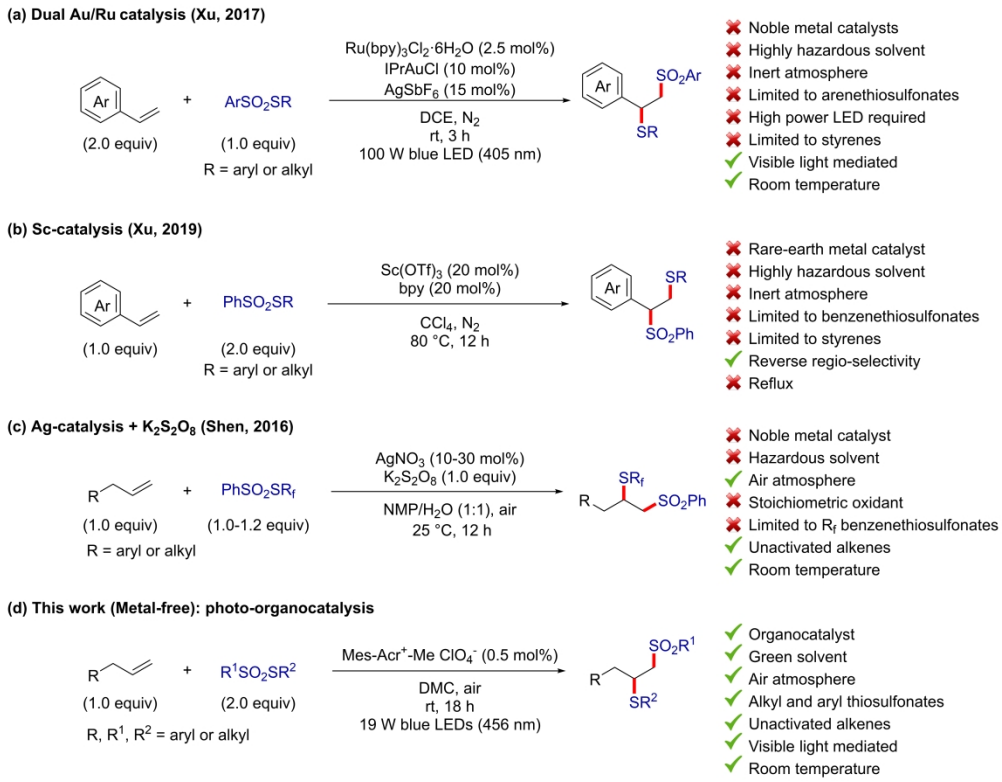

Scheme 1. Thiosulfonylation of alkenes: state-of-the-art metal catalysis versus organocatalysis.

223x174mm (600 x 600 DPI)

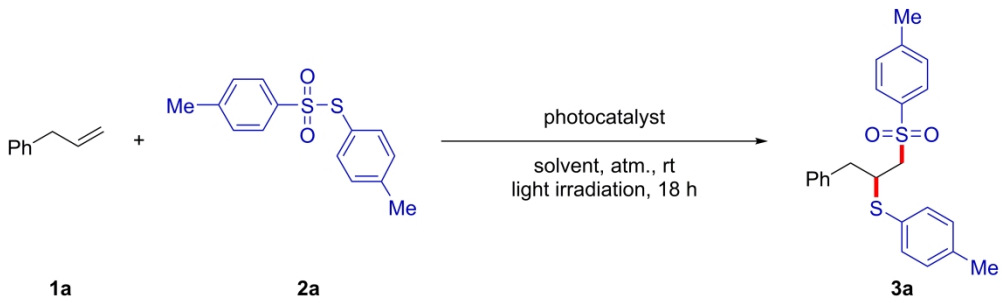

Table 1. Reaction optimization on the model reaction of allylbenzene (1a) with S-(4-methylphenyl) 4-methylbenzenethiosulfonate (2a).

171x51mm (600 x 600 DPI)

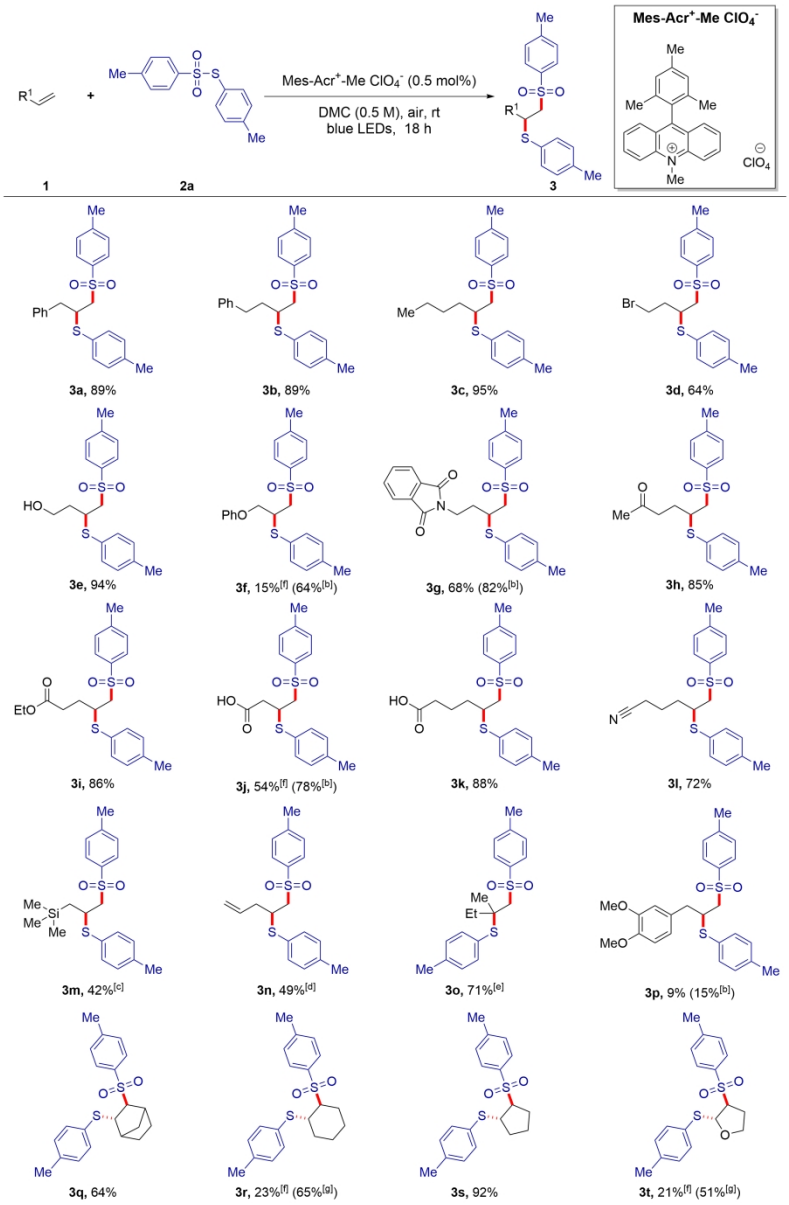

Table 2. Unactivated alkene (1) scope.

215x327mm (300 x 300 DPI)

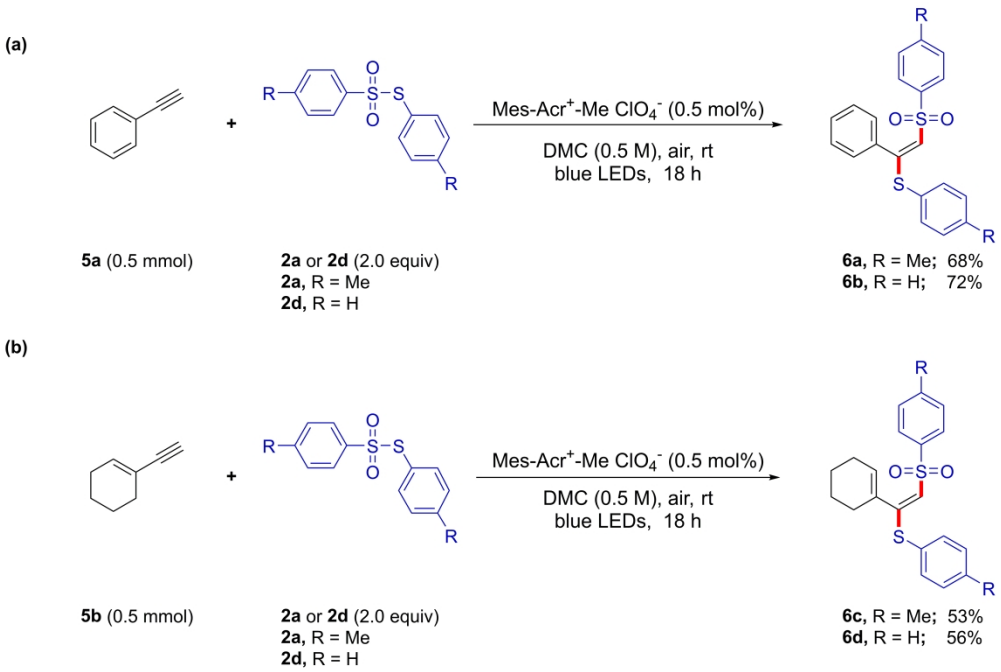

Scheme 2. Aromatic and aliphatic terminal alkynes (5a and 5b).

194x130mm (600 x 600 DPI)

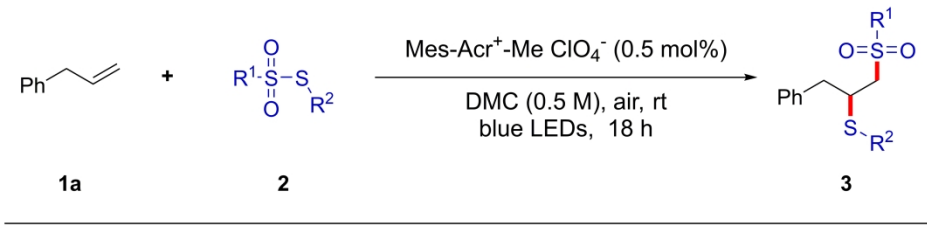

1a **2** **3**

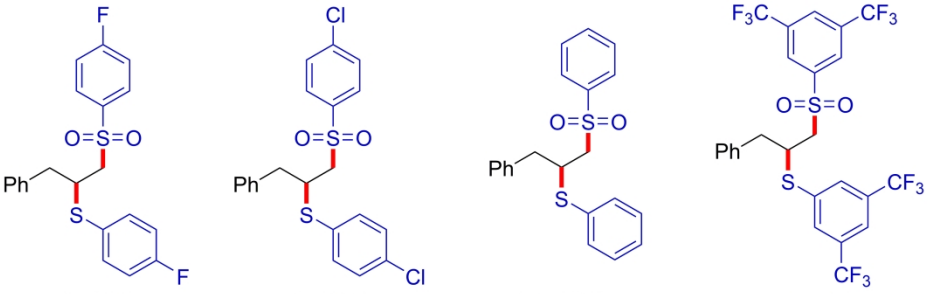

3u, 70% **3v,** 80% **3w,** 71% **3x,** 70%

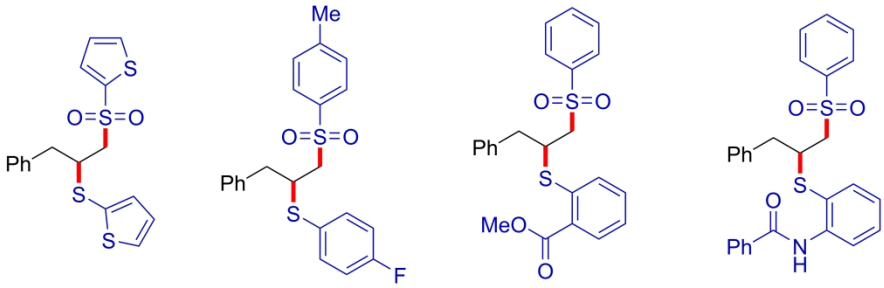

3y, 76% **3z,** 63% **3aa,** 84% **3ab,** 90%

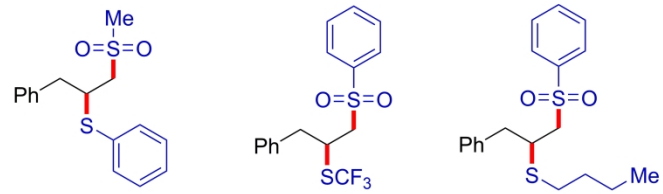

3ac, 13%[c] (72%[b]) **3ad,** 82% **3ae,** 0%

Table 3. Thiosulfonate (2) scope.

161x197mm (600 x 600 DPI)

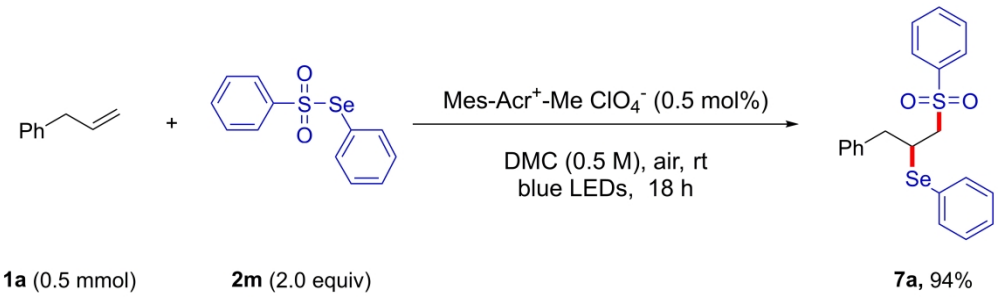

Scheme 3. Application of Se-phenyl benzeneselenosulfonate (2m)

162x48mm (600 x 600 DPI)

Scheme 4. 5-Exo-trig cyclization in 1,6-dienes (1u and 1v).

209x49mm (600 x 600 DPI)

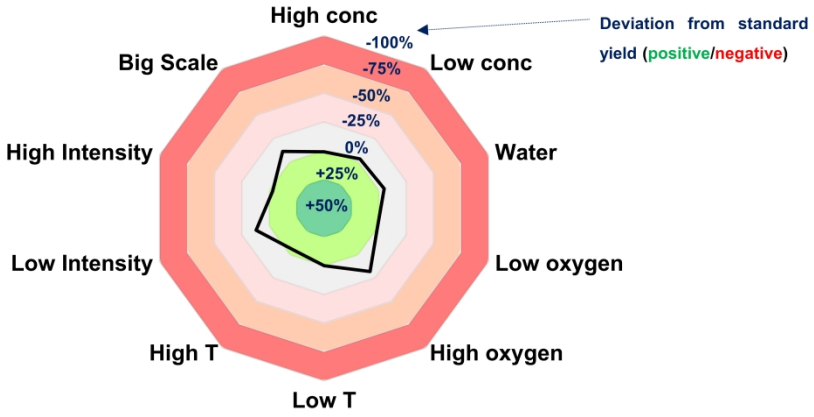

Figure 2. Sensitivity assessment of the developed reaction towards concentration, water level, oxygen level, temperature, light intensity and scale, illustrated via a color-coded radar diagram as proposed by Glorius et al.18 The deviation from standard reaction conditions is indicated as a black solid line. A round shape around the '0% deviation from standard line' indicates low sensitivity, any line deflecting from that to the red or green zones refer to high sensitivity of the reaction towards that parameter.

190x89mm (768 x 768 DPI)

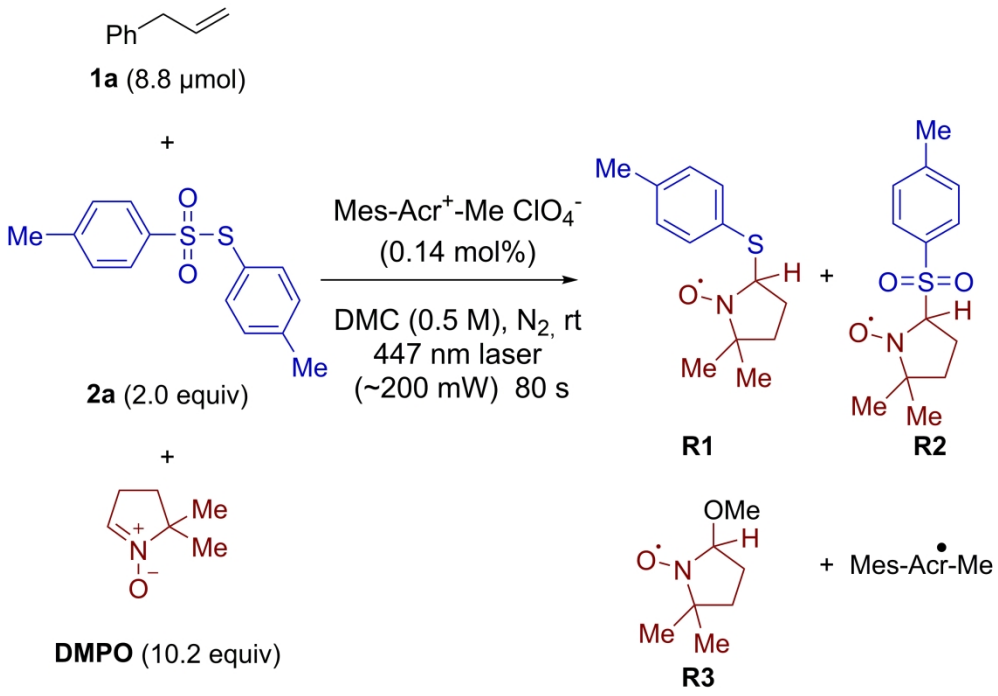

Figure 3. DMPO spin-trapping experiment on the model reaction of 1a and 2a, continuous wave (cw) X-band (~9.44 GHz) EPR recorded at room temperature using 5 mW microwave power, 0.05 mT modulation amplitude and 100 kHz modulation frequency, and the individual components used for the spectral simulations. The ratio of R1 : R2 : R3 : Mes-Acr˙-Me used for simulation was 1 : 0.9 : 0.6 : 6 (see SI section 6.9 for more details). Exp. = experimental spectrum. Sim. = simulated spectrum.

133x92mm (600 x 600 DPI)

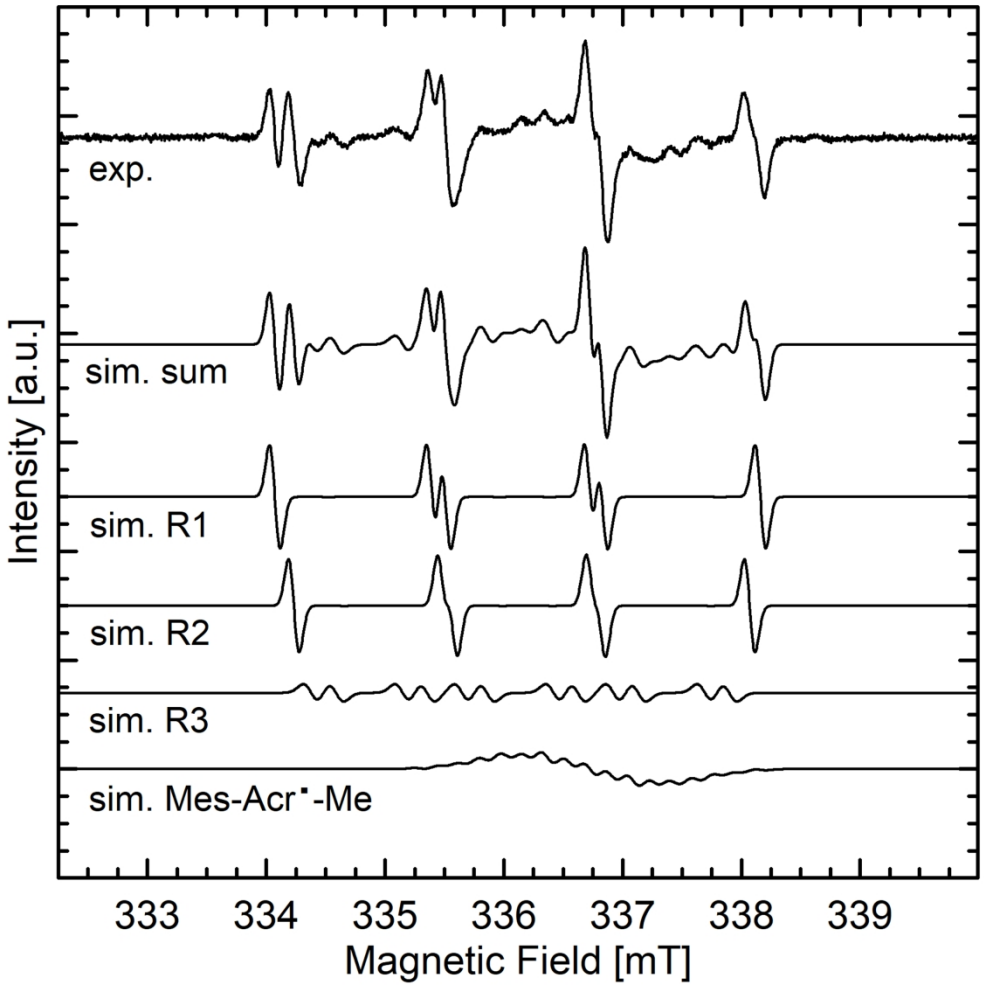

Figure 3. DMPO spin-trapping experiment on the model reaction of 1a and 2a, continuous wave (cw) X-band (~9.44 GHz) EPR recorded at room temperature using 5 mW microwave power, 0.05 mT modulation amplitude and 100 kHz modulation frequency, and the individual components used for the spectral simulations. The ratio of R1 : R2 : R3 : Mes-Acr˙-Me used for simulation was 1 : 0.9 : 0.6 : 6 (see SI section 6.9 for more details). Exp. = experimental spectrum. Sim. = simulated spectrum.

242x242mm (300 x 300 DPI)

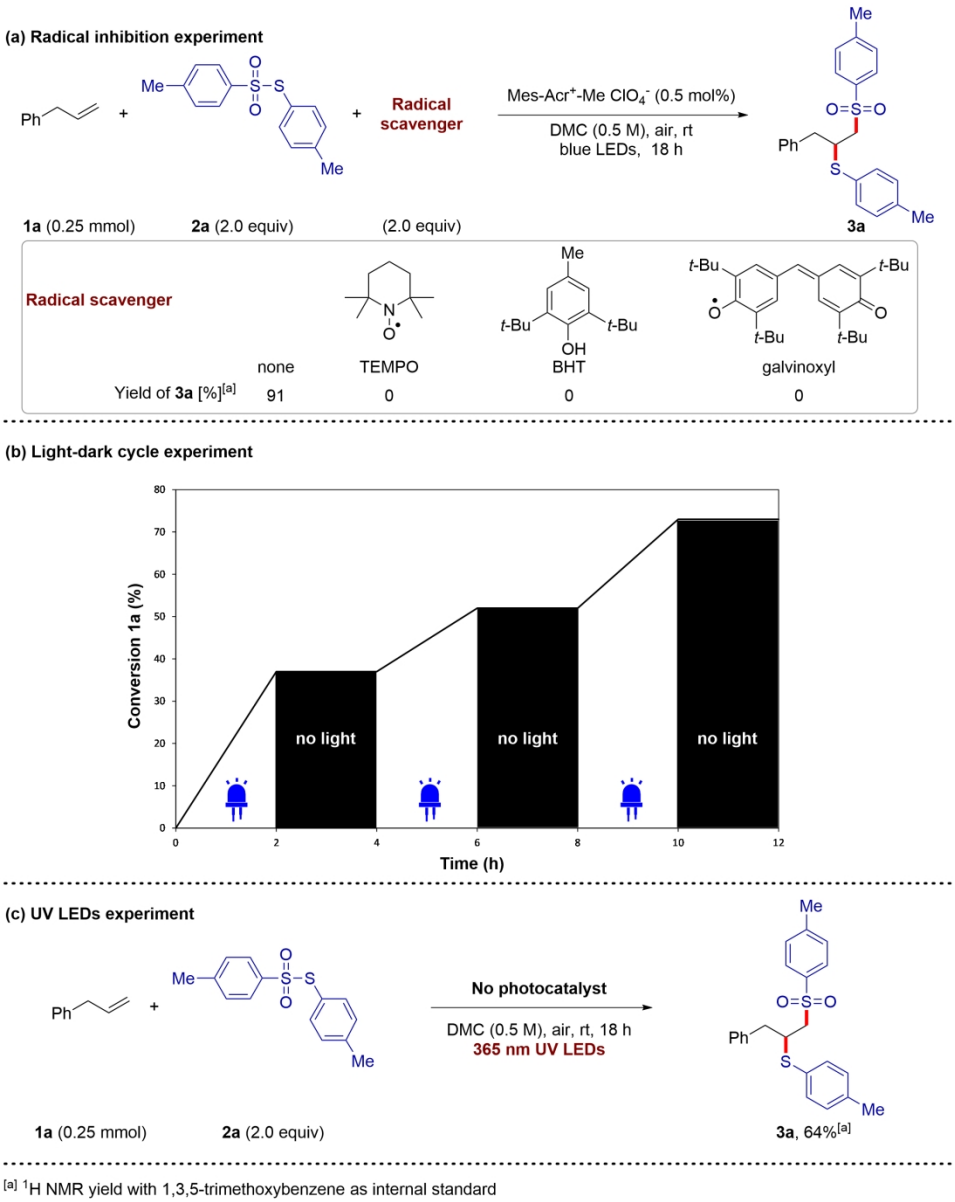

[a] ^{1}H NMR yield with 1,3,5-trimethoxybenzene as internal standard

Scheme 5. Control reactions to support mechanism.

201x253mm (300 x 300 DPI)

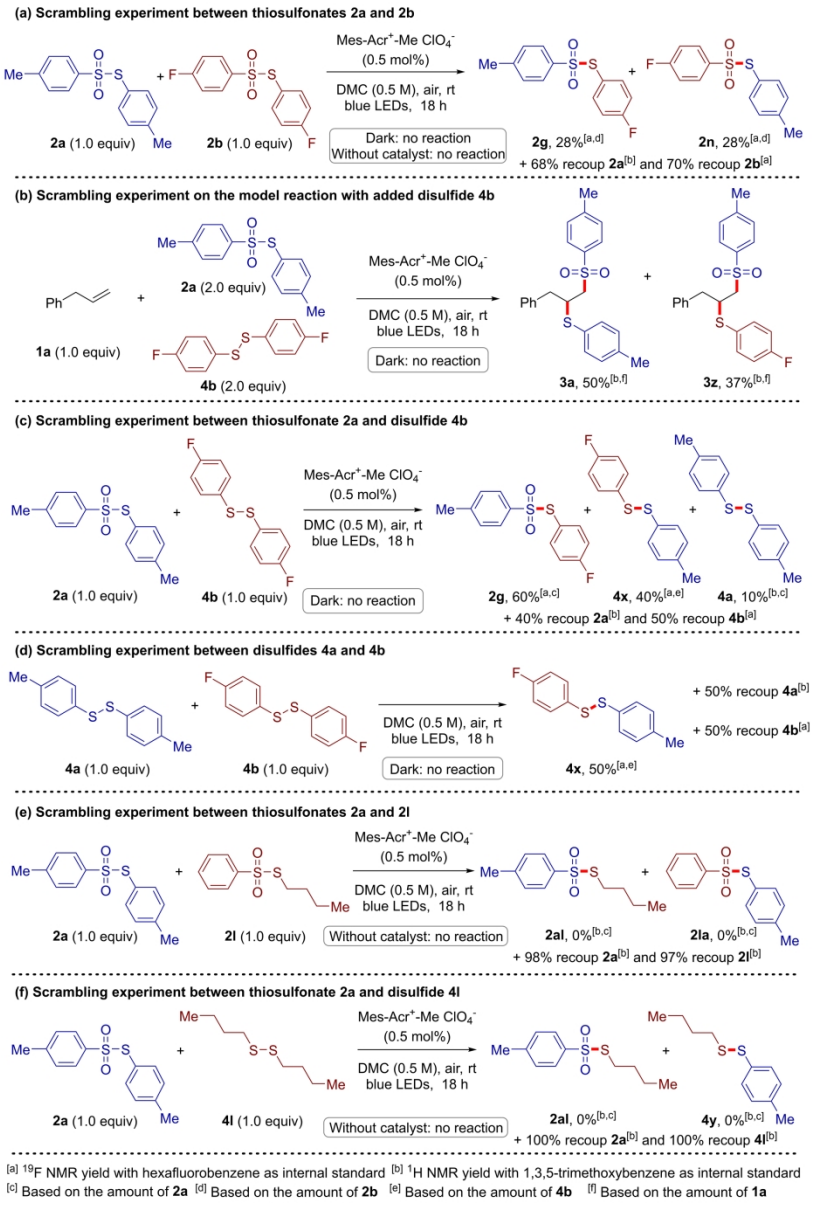

Scheme 6. Scrambling experiments to support the reaction mechanism.

207x305mm (300 x 300 DPI)

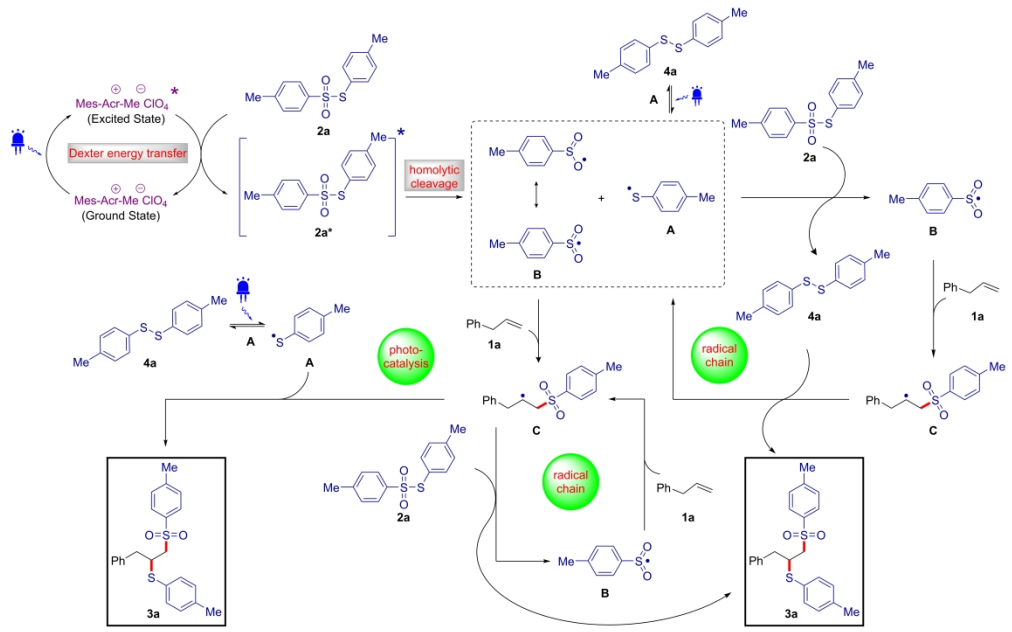

Scheme 7. Proposed reaction mechanism for the model reaction of 1a with 2a.

298x186mm (600 x 600 DPI)

Scheme 8. Gram-scale synthesis of 3a via thiosulfonylation of 1a with 2a.

228x55mm (300 x 300 DPI)

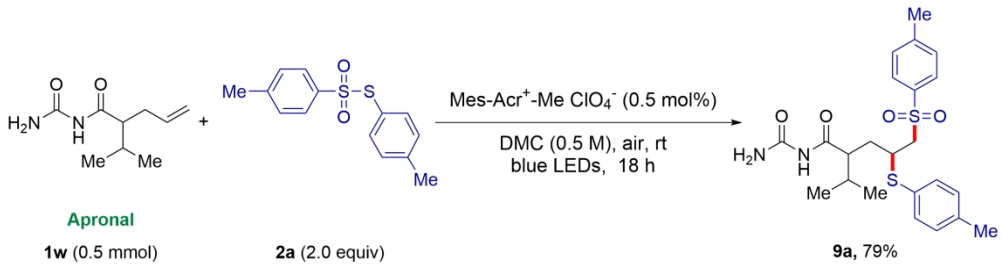

Scheme 9. Synthetic Applications: thiosulfonylation of API Apronal (1w) with thiosulfonate 2a.

197x52mm (300 x 300 DPI)

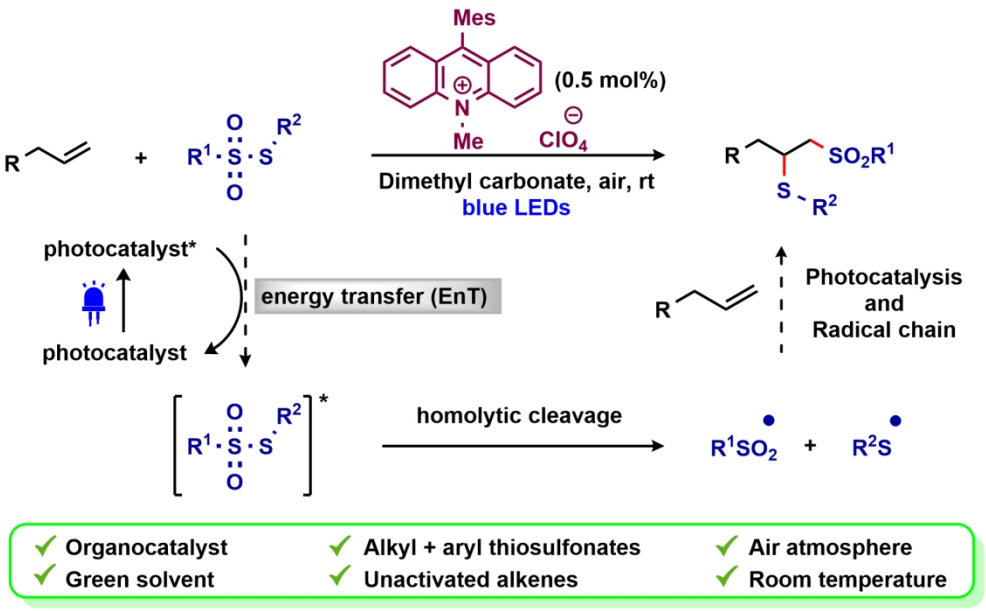

Table of content entry

79x49mm (600 x 600 DPI)